FACULTY OF SCIENCE
UNIVERSITY OF COPENHAGEN

Master Thesis

Unsupervised bilingual dictionary induction with stable GANs

Author: Xuwen Zhang `<dlv618@alumni.ku.dk>`

Supervisor: Anders Søgaard `<soegaard@di.ku.dk>`

Abstract

In machine translation, Generative adversarial networks (vanilla GAN) are the first approach to unsupervised cross-lingual word embedding alignment (CWEA) task, i.e., given two monolingual word embeddings, align them in the same space. There are other researchers who explored other improved GANs such as Wasserstein GAN on CWEA, but the WGAN with gradient penalty and CT-GAN have not been investigated on CWEA yet. In this thesis, we analyzed the performance of four different GANs, i.e, vanilla GAN, Wasserstein GAN, WGAN with gradient penalty and CT-GAN on CWEA, and show that in almost all situations, WGAN with gradient penalty not only obtained the best results but also the most robust and stable one compared to the other three.

Contents

Contents 3

1 Introduction 4
1.1 Background . . . 4
1.2 GANs and it's improved versions . . . 5

2 Vanilla GAN 8
2.1 Working mechanism . . . 8
2.2 Issues . . . 11

3 Wasserstein GAN 17
3.1 Several probability metrics . . . 17
3.2 Why is Wasserstain GAN better . . . 19
3.3 Wasserstein GAN . . . 23

4 Two improved WGANs 25
4.1 Wasserstein GAN with Gradient Penalty (WGAN-GP) . . . 25
4.2 Wasserstein GAN with A Consistency Term (CT-GAN) . . . 27

5 Experiments 29
5.1 data description . . . 29
5.2 Multilingual Unsupervised and Supervised Embeddings . . . 29
5.3 Experimental set up . . . 32
5.4 Results . . . 35

6 Discussion 43

A Some deep learning techniques 46
A.1 Layer normalization . . . 46
A.2 RMS prop . . . 47
A.3 Adam . . . 47
A.4 leaky Relu . . . 48

B Theorems which support proofs 49

Bibliography 50

Chapter 1

Introduction

1.1 Background

Word embedding is a way of representation for the vocabularies in a document, more specifically, it represents pieces of words as vectors. Word embedding can capture information about how different words are related to each other based on the context in a document. The most popular and powerful technique to learn word embeddings is called Word2Vec which is a shallow neural network, and it was introduced by Mikolov et al. (2013).

For given two monolingual language embeddings, i.e., a source embeddings and target embeddings, we can learn the cross-lingual word embeddings by mapping the source word embedding to the target embedding space to align both embeddings together in the same vector space. By Ruder et al. (2017), Cross-lingual word embeddings attract NLP researchers for two reasons:

- It enables computation of cross-lingual word similarities.
- Knowledge can be transferred between different languages, even transfer resource-rich language to resource-insufficient language like English to Finnish.

Broadly speaking, there are two methods to learn cross-lingual embeddings, supervised method and unsupervised method. Conneau et al.(2017) reviewed the supervised method at the beginning of their paper, then contributed a new unsupervised way to learn cross-lingual embeddings. In the supervised method, it assumed that for a given pair of language embeddings, a dictionary is given such that it would be used as an anchor point to align the two language embeddings. More specifically, assuming the dimension of both embeddings is d, X and Y are matrices with size $d \times n$, and the given dictionary contains n pairs of words $\{x_i, y_i\}_{i \in 1,2,\cdots,n}$ for $x_i \in X$ and $y_i \in Y$. Then this dictionary can be used to learn an optimal linear transformation W between X and Y such that

$$W^* = \underset{W}{\text{argmin}} \, \|WX - Y\|_F \tag{1.1}$$

where W is a $d \times d$ matrix, and $\|\cdot\|_F$ denotes the Frobenius norm. After the optimal transformation is obtained, for any source word s, the translation word

t in target embeddings can be found by searching for the nearest neighbor

$$t = \underset{t}{\text{argmax}} \cos(Wx_s, y_t).$$

The result of optimal W can be improved by orthogonalizing it (Xing et al. 2015). Thus, the equation (1.1) can be reformed to the Orthogonal Procrustes problem, and a solution would be reached by solving the singular value decomposition(SVD) of YX^T.

$$W^* = \underset{W}{\text{argmin}} \|WX - Y\|_F = UV^T,$$

Where $U\Sigma V^T = \text{SVD}(YX^T)$, the column vectors of U and V are orthonormal, and Σ is a diagonal matrix whose all diagonal elements are positive.

The unsupervised method which Conneau et al. proposed is like this:

- Assume two vector spaces are approximately isomorphic, i.e their exists an invertible linear mapping between them.
- Learn a rough approximation of mapping W by an adversarial model. In particular, by generative adversarial networks (GANs).
- Apply the learned mapping W to find word pairs for the most frequent words, and then refine W by Procrusters. The refined W would be used to translate all words in the embedding space.
- In the end, apply W to translate words by searching for the nearest neighbor score, and the nearest neighbor algorithm they used is called cross-domain similarity local scaling(CSLS), which invented by Conneau et al.

1.2 GANs and it's improved versions

Generative Adversarial Networks (GANs) are deep neural net architectures that consist of two networks, and GAN's development is considered a revolutionary advancement in deep learning. The original GANs which proposed by Goodfellow (Goodfellow et al., 2014)[3], it is called vanilla GAN. The idea of GANs was inspired by game theory, in which two networks are competing against each other, one is called generator, the other is discriminator, both networks will become more and more robust during the training process. More specifically,

- The discriminator is a binary classifier denoted as D which learns to recognize whether the input is coming from a real dataset or the generator's output. Formally, D calculates the probability of the sample coming from the generator G or the real input data for each iteration. Usually, in practice, the label defined as 1 for real samples and 0 for synthetic samples.

- The generator denoted as G, which takes random noise from the latent space and outputs synthetic samples. The training purpose for the generator is to approximate the distribution of real data as close as possible, at the same time the probability for fooling the discriminator would increase too, and this makes higher the probability that the discriminator would treat the synthetic output from the generator as real.

GANs are able to generate data from scratch based on the given sample. The main application area of GANs is computer vision, e.g., creating animated characters (Jin et al. 2017) which could be applied by game developing or animation production companies, high resolution images production based on given low resolution images (Ledig et al. 2016), and new video sequence generation (Vondrick et al. 2016).

GANs can also be applied to other domains such as music generation (Fedus et al. 2018), text generation (Mogren. 2016), or even text to image synthesis (Reed at el. 2016) etc. These applications show that GANs can be adapted immediately for commercial purpose.

Although GANs achieved great success, there are several disadvantages which makes GANs' training procedure unstable,

- Mode collapse happens frequently, which means the generator only learns limited distributions of real data.
- Lack of metric that can show the training process, therefore the training is fully manual.
- Gradient vanished, which means the generator's weights stop updating due to the discriminator performing too well.
- Highly sensitive for tuning hyperparameters.

Several improved versions of GANs attempt to solve the above issues, e.g, Wasserstain GAN (Arjovsky et al. 2017), in which the Earth Mover (Wasserstein) Distance is applied to substitute minimize the JS divergence as the new loss function due to the JS divergence would get stack at ln 2 in practice. But the calculation of Earth Mover Distance is intractable, therefore, the Kantorovich-Rubinstein duality (Villani. 2008) algorithm is applied, where all weights in the discriminator are constrained to a K-Lipschitz function, i.e., all weights in the discriminator must be clipped in a bounded interval. However, weight clipping will bring new issues, even Arjovsky pointed out in the original Wasserstein GAN paper that it is a horrible method to enforce a Lipschitz constraint.

Based on the issues of WGAN, there are new improved WGANs have been proposed, such as WGAN with gradient penalty (Gulrajani, et al. 2017). Instead of weight clipping, the gradient penalty term enforces Lipschitz by penalizing the norm of the discriminator's gradient. Our best models are obtained from this algorithm. Another improved WGANs is CT-GAN (Wei, et al. 2018), in which they claimed that the gradient penalty term not able to penalize all sample points, therefore they proposed a consistency term to be added to the WGAN with gradient penalty.

We focused on the unsupervised method which mentioned before in this thesis and do the following:

1. Reproduce the results of Conneau et al for several language pairs, and use the reproduced results as the baseline.
2. Implement the three improved GANs, and compare our result with the baseline. However, since we found that the WGAN-GP in the MUSE has the best performance, we focused on it mostly.
3. Analysing the results we obtained.

Chapter 2

Vanilla GAN

This chapter shows how Goodfellow et all interpret the mechanism of vanilla GAN, and some of the issues Arjovsky et al explored from vanilla GAN.

2.1 Working mechanism

In the training procedure of vanilla GAN, the training purpose for the generator G is to make the distribution of its output more and more close to real data, on the other hand, the goal of the discriminator D is to achieve a Nash equilibrium for which it is impossible to distinguish whether it's input comes from real or generated dataset. Formally speaking, the task of the discriminator D is to maximize

$$\mathbb{E}_{\boldsymbol{x}\sim\mathbb{P}_r(\boldsymbol{x})}[\log D(\boldsymbol{x})]$$

which means increasing the probability to identify samples coming from real data, as well as to reduce the probability $D(G(\boldsymbol{x}))$ to zero by maximizing

$$\mathbb{E}_{\boldsymbol{x}\sim\mathbb{P}_g(\boldsymbol{x})}[\log(1-D(G(\boldsymbol{x})))].$$

Thus, the objective function of the discriminator is

$$\max_D L(D) = \mathbb{E}_{\boldsymbol{x}\sim\mathbb{P}_r(\boldsymbol{x})}[\log D(\boldsymbol{x})] + \mathbb{E}_{\boldsymbol{z}\sim\mathbb{P}_g(\boldsymbol{z})}[\log(1-D(G(\boldsymbol{x})))].$$

At the same time, the task for training the generator G is to increase the value of probability of $D(G(\boldsymbol{x}))$, therefore the objective function of the generator is

$$\min_G L(G) = \mathbb{E}_{\boldsymbol{x}\sim\mathbb{P}_g(\boldsymbol{x})}[\log(1-D(G(\boldsymbol{x})))].$$

Since D and G are playing a mini-max game, the final objective function is

$$\min_G \max_D L(G,D) = \mathbb{E}_{\boldsymbol{x}\sim\mathbb{P}_r(\boldsymbol{x})}[\log D(\boldsymbol{x})] + \mathbb{E}_{\boldsymbol{z}\sim\mathbb{P}_g(\boldsymbol{z})}[(1-\log D(G(\boldsymbol{x})))]. \quad (2.1)$$

The notation $\mathbb{P}_r(\boldsymbol{x})$ means the probability distribution of real data, $\mathbb{P}_g(\boldsymbol{z})$ denotes generated fake data.

Proposition 2.1: [Proposition 1 (Goodfellow et all., 2014)]
For fixed G, the optimal value for D is:

$$D^*(\boldsymbol{x}) = \frac{p_r(\boldsymbol{x})}{p_r(\boldsymbol{x}) + p_g(\boldsymbol{x})}. \tag{2.2}$$

$Proof$:

Here is a summary of the proof by the original author:

Since the loss function in continuous probability distribution is

$$L(G, D) = \int_{\mathcal{X}} \Big(p_r(\boldsymbol{x})\log(D(\boldsymbol{x})) + p_{g(\boldsymbol{x})}\log(1 - D(\boldsymbol{x}))\Big) dx$$

the maximum value of $L(D, G)$ can be achieved by solving the function inside the integral. For convenience, define the function inside the integral as

$$f(y) = p_r(x)\log y + p_g(x)\log\big(1 - y\big),$$

and take the derivative of loss with respect to x and set it to zero, then get

$$\begin{aligned} \frac{df(y)}{dy} &= p_r(x)\frac{1}{y} - p_g(x)\frac{1}{1-y} \\ &= \frac{p_r(x) - y\big(p_r(x) + p_g(x)\big)}{y(1-y)} \\ &= 0 \\ \Longrightarrow y &= \frac{p_r(x)}{p_r(x) + p_g(x)} \end{aligned}$$

Apply the above to a vector variable x.
Thus, the $D^*(\boldsymbol{x}) = \frac{p_r(\boldsymbol{x})}{p_r(\boldsymbol{x})+p_g(\boldsymbol{x})} \in [0, 1]$. □

By Proposition 2.1 above, The equation (2.1) can be rewritten as

$$\begin{aligned} L(G, D^*) &= \max_D L(G, D) \\ &= \mathbb{E}_{\boldsymbol{x}\sim\mathbb{P}_r}[\,\log D^*(\boldsymbol{x})] + \mathbb{E}_{\boldsymbol{x}\sim\mathbb{P}_g}[(1 - \log D^*(\boldsymbol{x}))\,] \\ &= \mathbb{E}_{\boldsymbol{x}\sim\mathbb{P}_r}\Big[\frac{p_r(\boldsymbol{x})}{p_r(\boldsymbol{x}) + p_g(\boldsymbol{x})}\Big] + \mathbb{E}_{\boldsymbol{x}\sim\mathbb{P}_g}\Big[\frac{p_g(\boldsymbol{x})}{p_r(\boldsymbol{x}) + p_g(\boldsymbol{x})}\Big] \end{aligned}$$

Theorem 2.1: [Theorem 1 (Goodfellow et all., 2014)]

The global minimum of $L(G, D^*)$ can be reached if and only if $p_r(\boldsymbol{x}) = p_g(\boldsymbol{x})$. And at this moment, $L(G, D^*) = -2\log 2$ and $D^*(\boldsymbol{x}) = 0.5$.

Proof:

Here is a summary of the proof by the original author:

By equation (2.2), if $p_r(\boldsymbol{x}) = p_g(\boldsymbol{x})$, then $D^*(\boldsymbol{x}) = 0.5$, substituting this value to equation (4) we have

$$\begin{aligned}\min_G L(G, D^*) &= \int_{\mathcal{X}} \Big(p_r(\boldsymbol{x})\log\frac{1}{2} + p_{g(\boldsymbol{x})}\log\frac{1}{2}\Big)dx\\ &=\log\frac{1}{2}\Big(\int_{\mathcal{X}} p_r(\boldsymbol{x})dx + \int_{\mathcal{X}} p_{g(\boldsymbol{x})}dx\Big)\\ &=2\log\frac{1}{2}\\ &=-2\log2.\end{aligned}$$

to show $-2\log2$ is the optimal value for $L(G, D^*)$, we need to prove they are equal to each other. Subtracting one from the other and by applying proposition 1 we get

$$\begin{aligned}L(G, D^*) - \big(-2\log2\big) =& 2\log2 + \int_{\mathcal{X}} \Big(p_r(\boldsymbol{x})\,\log\frac{p_r(\boldsymbol{x})}{p_r(\boldsymbol{x}) + p_g(\boldsymbol{x})}\\ &+p_g(\boldsymbol{x})\,\log\frac{p_g(\boldsymbol{x})}{p_r(x) + p_g(\boldsymbol{x})}\Big)dx\\ =&\Big(\log2 + \int_{\mathcal{X}} p_r(\boldsymbol{x})\,\log\frac{p_r(\boldsymbol{x})}{p_r(\boldsymbol{x}) + p_g(\boldsymbol{x})}dx\Big)\\ &+\Big(\log2 + \int_{\mathcal{X}} p_g(\boldsymbol{x})\,\log\frac{p_g(\boldsymbol{x})}{p_r(\boldsymbol{x}) + p_g(\boldsymbol{x})}dx\Big)\\ =&\Big(\int_{\mathcal{X}} p_r(\boldsymbol{x})\log2\,dx + \int_{\mathcal{X}} p_r(\boldsymbol{x})\,\log\frac{p_r(\boldsymbol{x})}{p_r(\boldsymbol{x}) + p_g(\boldsymbol{x})}dx\Big)\\ &+\Big(\int_{\mathcal{X}} p_g(\boldsymbol{x})\log2\,dx + \int_{\mathcal{X}} p_g(\boldsymbol{x})\,\log\frac{p_g(\boldsymbol{x})}{p_r(\boldsymbol{x}) + p_g(\boldsymbol{x})}dx\Big)\\ =&\int_{\mathcal{X}} p_r(\boldsymbol{x})\log\frac{2\cdot p_r(\boldsymbol{x})}{p_r(\boldsymbol{x}) + p_g(\boldsymbol{x})}dx + \int_{\mathcal{X}} p_g(\boldsymbol{x})\log\frac{2\cdot p_g(\boldsymbol{x})}{p_r(\boldsymbol{x}) + p_g(\boldsymbol{x})}dx\\ =&KL\Big(p_r||\frac{p_r + p_g}{2}\Big) + KL\Big(p_g||\frac{p_r + p_g}{2}\Big)\\ =&2JS(p_r||p_g)\end{aligned}$$

Since the Jensen-Shannon divergence equals to zero when the two probability distributions p_r and p_g are equal everywhere, then, the global optimal value for the loss is - 2 log2 and $D^*(\boldsymbol{x}) = 0.5$. □

Below is the architecture draft of vanilla GAN and the training algorithm in the original paper (Goodfellow et all., 2014)[3].

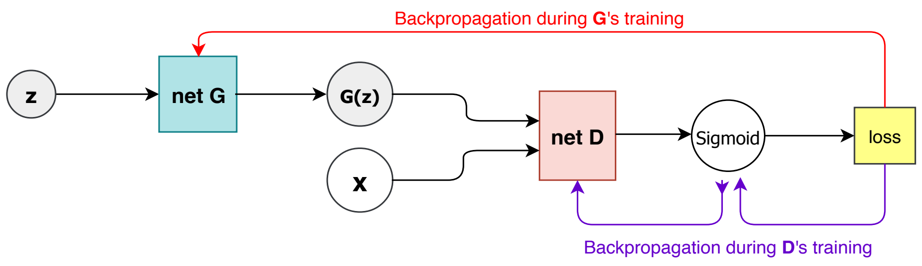
Backpropagation during G's training
z
net G
G(z)
x
net D
Sigmoid
loss
Backpropagation during D's training

Figure 2.1: The structure of Vanilla GAN

Algorithm 2.1: Minbatch training algorithm uses stochastic gradient descent as optimizer, n is a hyperparameter which for each generator's iteration, trains discriminator D for n iterations. The original paper used $n = 1$.

```
1: for i = 1, 2, ..., number of training iterations do
2:     for training discriminator $n$ iterations do
3:         Sample $k$ minibatch random noise from latent space distribution $p_g(\boldsymbol{z})$
4:         Sample $k$ minibatch input examples from data distribution $p_r(\boldsymbol{x})$
5:         Backpropagating all weights in $D$ by maximizing the loss:
               $$\nabla_{W_D} \frac{1}{k} \sum_{i=1}^{k} \left[ \log D(\boldsymbol{x}^{(i)}) + \log \left(1 - D\big(G(\boldsymbol{z}^{(i)})\big)\right) \right].$$
6:     end for
7:     Sample $k$ minibatch random noise from latent space distribution $p_g(\boldsymbol{z})$
8:     Backpropagating all weights in $G$ by minimizing the loss:
           $$\nabla_{W_G} \frac{1}{k} \sum_{i=1}^{k} \log \left(1 - D\big(G(\boldsymbol{z}^{(i)})\big)\right).$$
9: end for
```

However, Goodfellow et all pointed out that in practice, when the training has just started, the distributions of $\mathbb{P}_r$ and $\mathbb{P}_g$ may have a huge difference, in this case, D can easily distinguish whether the data comes from training data or synthetic. Therefore, $\log\big(1 - D(G(\boldsymbol{z}))\big)$ saturates. Maximizing $\log D(G(\boldsymbol{z}))$ for generator can provide more robust gradients in the early training instead of minimizing $\log\big(1 - D(G(\boldsymbol{z}))\big)$.

2.2 Issues

By Theorem 2.1, the minimum of the discriminator's loss is

$$L(G, D^*) = 2JS(\mathbb{P}_r||\mathbb{P}_g) - 2\log 2$$

where $JS(\mathbb{P}_r||\mathbb{P}_g)$ as close to 0 as possible. However, the discriminator's loss will converge to zero in practice, and this means that $JS(\mathbb{P}_r||\mathbb{P}_g)$ will converge to ln 2 instead of zero.

By Arjovsky et al [19], the reasons which prevent $JS(\mathbb{P}_r||\mathbb{P}_g)$ converge to zero is that

- Either the distributions are discontinuous, in other words, the probability density function does not exist.
- Or both distributions have disjoint supports.

There is a possible reason which makes the distributions discontinuous, that is, both of their supports to lie on lower dimensional manifolds.

Narayanan et al. (2010) claimed that the support of the distribution of $\mathbb{P}_r$ lies on a low dimensional manifold. For $\mathbb{P}_g$, if dim($\mathcal{Z}$) < dim($\mathcal{X}$), then $\mathbb{P}_g$ is not continuous. This concept is mathematically formalized in the following lemma:

Lemma 2.1: [Lemma 1. (Arjovsky et al. 2017)] Assume $g : \mathcal{Z} \mapsto \mathcal{X}$ be a neural network, which is a function composed by affine transformations with non-linear activation functions, then a countable union of manifolds which contains $g(\mathcal{Z})$ would have dimension less than or equal to dim($\mathcal{Z}$). Thus, the measure of $g(\mathcal{Z})$ would be zero in $\mathcal{X}$ if dim($\mathcal{Z}$) < dim($\mathcal{X}$).

Since the generator G is a neural network, this lemma states that if the input dimension of $\boldsymbol{z}$ is less than $g(\boldsymbol{z})$, then the learning ability of $g(\boldsymbol{z})$ will be limited, only a small part of the input of the distribution can be learned by $g(\boldsymbol{z})$ due to the zero measure of $g(\boldsymbol{z})$.

The next theorem states that if the supports of two distributions $\mathbb{P}_r$ and $\mathbb{P}_g$ are disjoint, there exists a perfect discriminator, along with vanishing gradients. In this case, when D trained too well, G's weights stop updating and make G to stop approximating.

Theorem 2.3: [Theorem 2.1 (Arjovsky et al. 2017)]
Assume the supports of $\mathbb{P}_r$ and $\mathbb{P}_g$ are included on disjoint compact subsets $\mathcal{M}$ and $\mathcal{S}$ respectively, then there exists a completely accurate smooth discriminator $D^* : \mathcal{X} \mapsto [0, 1]$ which has 0 error, plus $\nabla_{\boldsymbol{x}} D^*(\boldsymbol{x}) = 0, \ \forall \boldsymbol{x} \in \mathcal{M} \cup \mathcal{S}$.

$Proof$:

Here is a summary of the proof by the original author:

By assumption, $\mathcal{M}$ and $\mathcal{S}$ are disjoint and compact. Supposed $d(\mathcal{M}, \mathcal{S}) =$

$\epsilon > 0$ is the distance between $\mathcal{M}$ and $\mathcal{S}$, then define another two sets

$$\mathcal{M}' = \{\boldsymbol{x} : d(\boldsymbol{x}, \mathcal{M}) \leq \frac{\epsilon}{3}\}$$
$$\mathcal{S}' = \{\boldsymbol{x} : d(\boldsymbol{x}, \mathcal{S}) \leq \frac{\epsilon}{3}\}$$

therefore $\mathcal{M}'$ and $\mathcal{S}'$ are also both disjoint and compact. Thus, by applying Smooth Urysohn's Lemma, exists a continuous function $D^* : \mathcal{X} \mapsto [0, 1]$ such that $D^*\big|_{\mathcal{S}'} \equiv 0$ and $D^*\big|_{\mathcal{M}'} \equiv 1$. Since $\forall \boldsymbol{x} \in \text{supp}(D^*\big|_{\mathbb{P}_r}) = \{\boldsymbol{x} \in \mathbb{P}_r \big| D^* \neq 0\}$, $\log D^*(\boldsymbol{x}) = 0$, and $\log\big(1 - D^*(\boldsymbol{x})\big) = 0 \ \forall \boldsymbol{x} \in \text{supp}(D^*\big|_{\mathbb{P}_g})$, therefore the discriminator has zero error and has become optimal. In addition, for proving $D^*(\boldsymbol{x}) = 0$, first define $\boldsymbol{x} \in \mathcal{M} \cup \mathcal{S}$, then for $\boldsymbol{x} \in \mathcal{M}$, there exists an open ball $\mathcal{B}(\boldsymbol{x}, \frac{\epsilon}{3}) = \mathcal{B}'$ such that $D^*\big|_{\mathcal{B}'}$ is constant. Thus $\nabla_{\boldsymbol{x}} D^* \equiv 0$. For $\boldsymbol{x} \in \mathcal{S}$, following the same procedure will finish the proof. $\square$

This theorem says, if the intersection of the supports of $\mathbb{P}_r$ and $\mathbb{P}_g$ is empty, then there exists a perfect discriminator which is able to separate $\mathbb{P}_r$ and $\mathbb{P}_g$, and D's gradient with respect to $\boldsymbol{x}$ will be vanished on the union of the two supports. This makes G stop learning when D trained too well.

Definition 2.1: (Transversal intersection) [Definition 2.2 (Arjovsky et al. 2017)]
Assume $\mathcal{M}$ and $\mathcal{S}$ are two submanifolds of $\mathcal{F}$, and $\mathcal{F} = \mathbb{R}^n$. If $\forall p \in \mathcal{M} \cap \mathcal{S}$

$$T_p\mathcal{M} + T_p\mathcal{S} = T_pF$$

then we say that $\mathcal{M}$ and $\mathcal{S}$ intersect transversally.

$T_p\mathcal{M}$ means the tangent space of $\mathcal{M}$ at point p. Moreover, if two submanifolds have intersection at a point, then they are non-transversal.

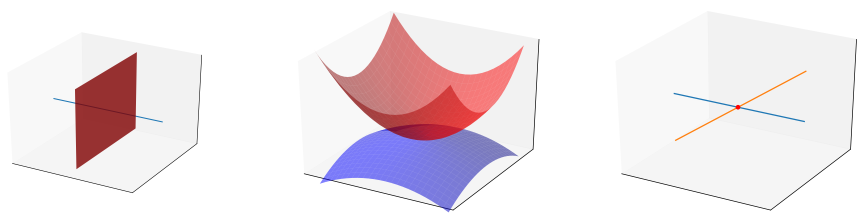

(a) transverse (b) non-transverse (c) non-transverse

Figure 2.2: examples of transversal intersection

Definition 2.2: (Perfect align) [Definition 2.2 (Arjovsky et al. 2017)] Assume $\mathcal{M}$ and $\mathcal{S}$ are two manifolds without boundary. We say $\mathcal{M}$ and $\mathcal{S}$ perfectly align if there exists $\boldsymbol{x} \in \mathcal{M} \cap \mathcal{S}$ such that $\mathcal{M}$ and $\mathcal{S}$ are non-transversal at $\boldsymbol{x}$.

Lemma 2.2: [Lemma 2. (Arjovsky et al. 2017)]
Assume $\mathcal{M}$ and $\mathcal{S}$ are two regular submanifolds of $\mathbb{R}^n$, and they do not have a full dimension. Suppose ϵ and ϵ' are two independent continuous random variables, defining two perturbed manifolds $\hat{\mathcal{M}} = \mathcal{M} + \epsilon$ and $\hat{\mathcal{S}} = \mathcal{S} + \epsilon'$. Then

$$\mathbb{P}_{\epsilon,\epsilon'}\big(\hat{\mathcal{M}} \text{ and } \hat{\mathcal{S}} \text{ not perfectly align }\big) = 1.$$

This lemma means that any small perturbations can make two low dimension manifolds become non-perfectly aligned, i.e., transversally intersect.

Lemma 2.3: [Lemma 3. (Arjovsky et al. 2017)]
Assume $\mathcal{M}$ and $\mathcal{S}$ are two non-full dimension and non-perfectly aligned regular submanifolds of $\mathbb{R}^n$. Let $\mathcal{M} \cap \mathcal{S} = \mathcal{P}$.

- If $\mathcal{M}$ and $\mathcal{S}$ have boundary, then $\mathcal{P}$ is a union of no more than four strictly low dimensional manifolds.
- If $\mathcal{M}$ and $\mathcal{S}$ without boundary. then $\mathcal{P}$ is still a manifold which has strictly lower dimension than $\mathcal{M}$ or $\mathcal{S}$.

$\mathcal{P}$ has measure zero in $\mathcal{M}$ and $\mathcal{S}$ in both cases.

By Lemma 2.2, two manifols can be non-perfectly aligned by any subtle disturbation, therefore by Lemma 2.3, their intersection has zero measure.

Theorem 2.4: [Theorem 2.2 (Arjovsky et al. 2017)]
Assume $\mathbb{P}_r$ and $\mathbb{P}_g$ are two distributions, their supports contained respectively in two closed lower dimensional manifolds $\mathcal{M}$ and $\mathcal{S}$ which are non-perfectly aligned. In addition, suppose $\mathbb{P}_r$ and $\mathbb{P}_g$ are continuous, which means that for any set $A \in \mathcal{M}$ with zero measure it is $\mathbb{P}_r\big(A\big) = 0$, similar for $\mathbb{P}_g$. Then there is an full accuracy optimal discriminator $D^* : \mathcal{X} \mapsto [0, 1]$ which can distinguish $\mathbb{P}_r$ and $\mathbb{P}_g$. Moreover, $\forall \boldsymbol{x} \in \mathcal{M}$ or $\forall \boldsymbol{x} \in \mathcal{S}$, $\nabla_{\boldsymbol{x}} D^*(\boldsymbol{x}) = 0$ and D^* is smooth in a neighborhood.

In Theorem 2.3, we assumed that the supports of both $\mathcal{M}$ and $\mathcal{S}$ are disjoint. However Theorem 2.4 says, even in the condition that the supports of $\mathcal{M}$ and $\mathcal{S}$ are joint and non-perfectly aligned,there still exists a perfect discriminator which can separate $\mathcal{M}$ and $\mathcal{S}$, which also makes the generator's gradient vanish.

Theorem 2.5: [Theorem 2.3 (Arjovsky et al. 2017)]
Assume $\mathbb{P}_r$ and $\mathbb{P}_g$ are two distributions, their supports contained respectively in two lower dimensional manifolds $\mathcal{M}$ and $\mathcal{S}$ which are non-perfectly aligned. Furthermore, assume $\mathbb{P}_r$ and $\mathbb{P}_g$ are continuous in their manifolds. Then

- $JSD\big(\mathbb{P}_r \| \mathbb{P}_g\big)$ = ln 2
- $KL\big(\mathbb{P}_r \| \mathbb{P}_g\big) = +\infty$
- $KL\big(\mathbb{P}_g \| \mathbb{P}_r\big) = +\infty$

This theorem indicates that under the same condition of Theorem 2.4, a perfect discriminator can be trained, then the Jensen Shannon divergence between two distributions will get close to ln2. In addition, KL divergence is not available as a metric to evaluate GANs' performance, thus finding a useful metric is the new goal.

Theorem 2.6: [Theorem 2.4 (Arjovsky et al. 2017)]
Assume $g_\theta : Z \mapsto \mathcal{X}$ is a differentiable function which induce the distribution $\mathbb{P}_g$ and let $\mathbb{P}_r$ be the input data distribution. Let D be a differentiable discriminator. If the conditions in Theorem 2.3 and 2.4 are satisfied, $\mathbb{E}_{\boldsymbol{z}\sim p(\boldsymbol{z})}\big[\|J_\theta g_\theta(z)\|_2^2\big] \leq M^2$ and $\|D - D^*\| < \epsilon$, then

$$\big\|\nabla_\theta \mathbb{E}_{\boldsymbol{z}\sim p(\boldsymbol{z})}\big[\log\big(1 - D(g_\theta(\boldsymbol{z}))\big)\big]\big\|_2 < M\frac{\epsilon}{1-\epsilon}$$

Proof:

Here is a summary of the proof by the original author:

Since the conditions from Theorem 2.3 and 2.4 satisfied, $\nabla_{\boldsymbol{x}} D^*(\boldsymbol{x}) = 0$ is locally on $\mathbb{P}_g$. Therefore, by Jensen's inequality and the chain rule

$$\begin{aligned}
\big\|\nabla_\theta \mathbb{E}_{\boldsymbol{z}\sim p(\boldsymbol{z})}\big[\log\big(1 - D(g_\theta(\boldsymbol{z}))\big)\big]\big\|_2^2 &\leq \mathbb{E}_{\boldsymbol{z}\sim p(\boldsymbol{z})}\Big[\frac{\|\nabla_\theta D\big(g_\theta(\boldsymbol{z})\big)\|_2^2}{|1 - D\big(g_\theta(\boldsymbol{z})\big)|^2}\Big] \\
&= \mathbb{E}_{\boldsymbol{z}\sim p(\boldsymbol{z})}\Big[\frac{\|J_\theta g_\theta(\boldsymbol{z})\nabla_{\boldsymbol{x}} D\big(g_\theta(\boldsymbol{z})\big)\|_2^2}{|1 - D\big(g_\theta(\boldsymbol{z})\big)|^2}\Big] \\
&\leq \mathbb{E}_{\boldsymbol{z}\sim p(\boldsymbol{z})}\Big[\frac{\|\nabla_{\boldsymbol{x}} D\big(g_\theta(\boldsymbol{z})\big)\|_2^2\|J_\theta g_\theta(\boldsymbol{z})\|_2^2}{|1 - D\big(g_\theta(\boldsymbol{z})\big)|^2}\Big] \\
&\leq \mathbb{E}_{\boldsymbol{z}\sim p(\boldsymbol{z})}\Big[\frac{\big(\|\nabla_{\boldsymbol{x}} D^*\big(g_\theta(\boldsymbol{z})\big)\|_2 + \epsilon\big)^2\|J_\theta g_\theta(\boldsymbol{z})\|_2^2}{\big(|1 - D^*\big(g_\theta(\boldsymbol{z})\big)| - \epsilon\big)^2}\Big] \\
&= \mathbb{E}_{\boldsymbol{z}\sim p(\boldsymbol{z})}\Big[\frac{\epsilon^2\|J_\theta g_\theta(\boldsymbol{z})\|_2^2}{\big(1-\epsilon\big)^2}\Big] \\
&\leq M^2\frac{\epsilon^2}{(1-\epsilon)^2}
\end{aligned}$$

After taking the square root of each side, we get the final result

$$\big\|\nabla_\theta \mathbb{E}_{\boldsymbol{z}\sim p(\boldsymbol{z})}\big[\log\big(1 - D(g_\theta(\boldsymbol{z}))\big)\big]\big\|_2 < M\frac{\epsilon}{1-\epsilon}$$

□

Corollary 2.1: [Corollary 2.1 (Arjovsky et al. 2017)]
Assume all conditions from Theorem 6 are satisfied, then

$$\lim_{\|D-D^*\|\to 0} \nabla_\theta \mathbb{E}_{\boldsymbol{z}\sim p(\boldsymbol{z})}\big[\log\big(1 - D(g_\theta(\boldsymbol{z}))\big)\big] = 0$$

The Theorem 2.6 and Corollary 2.1 the generator's gradient is bounded, in other words,the more close the discriminator D is to it's optimal, the smaller the gradient of the generator is. Therefore, in this situation, the generator stops learning the input distribution .

Chapter 3

Wasserstein GAN

The way vanilla GAN works and why it's hard to train has already shown up in the previous chapter. Arjovsky et al.(2017) first reviewed several metrics which for measure two given probability distributions, then applied the Earth Mover Distance(EMD) to introduce a new GAN called Wasserstein GAN which tries to solve them, e.g., mode collapse, and lack of metric that informs us about the training progress. However, even though Wasserstein GAN has better performance than vanilla GAN in image generation, it still has some flaws such as weight clipping.

3.1 Several probability metrics

There are several formulas to measure the similarity between two probability distributions over the same random variable x. Assume $\mathbb{P}_r(\boldsymbol{x})$ and $\mathbb{P}_g(\boldsymbol{x})$ are two distributions, $P_r(\boldsymbol{x})$ and $P_g(\boldsymbol{x})$ are the corresponding density functions.

Kullback-Leibler (KL) divergence:

The continuous form of KL divergence is defined as

$$KL(\mathbb{P}_r||\mathbb{P}_g) = \int_{\mathcal{X}} \log\Big(\frac{P_r(\boldsymbol{x})}{P_g(\boldsymbol{x})}\Big) P_r(\boldsymbol{x}) d\boldsymbol{x},$$

it's lower bounded by 0. KL Divergence reaches minimum zero while $P_r(x) = P_g(x)$ for all $x \in \mathcal{X}$. In addition, the discrete form of KL divergence is :

$$\begin{aligned} KL(\mathbb{P}_r||\mathbb{P}_g) =& H(p) - H(p,q) \\ =& \sum_x \log\Big(\frac{P_r(\boldsymbol{x})}{P_g(\boldsymbol{x})}\Big) P_r(\boldsymbol{x}) \\ =& -\sum_x \log\Big(\frac{P_g(\boldsymbol{x})}{P_r(\boldsymbol{x})}\Big) P_r(\boldsymbol{x}), \end{aligned}$$

where $H(p,q)$ is the cross entropy between p and q. KL divergence is asymmetric.

Jensen-Shannon (JS) divergence:

$$JS(\mathbb{P}_r, \mathbb{P}_g) = \frac{1}{2} KL(\mathbb{P}_r || \mathbb{P}_m) + \frac{1}{2} KL(\mathbb{P}_g || \mathbb{P}_m)$$

where $\mathbb{P}_m = \frac{\mathbb{P}_r + \mathbb{P}_g}{2}$. The JS divergence is bounded in $[0, 1]$, and it is symmetric, i.e. $JS(\mathbb{P}_r, \mathbb{P}_g) = JS(\mathbb{P}_g, \mathbb{P}_r)$.

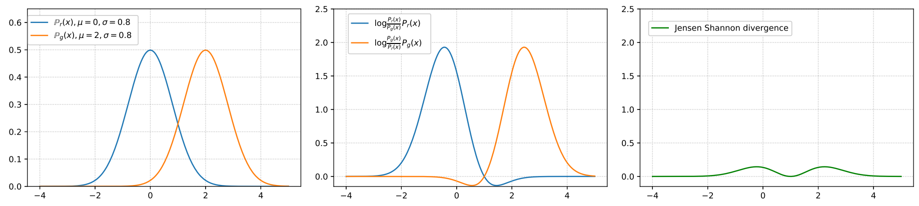

(a) $\mathbb{P}_r(\mathcal{X})$ and $\mathbb{P}_g(\mathcal{X})$ (b)$KL(\mathbb{P}_r || \mathbb{P}_g)$ and $KL(\mathbb{P}_g || \mathbb{P}_r)$ (c) Jensen Shannon divergence

Figure 3.1: Two different normal distributions with corresponding KL and JSD

Earth Mover Distance (EMD):

The last metric they reviewed is the Earth Mover's Distance (EMD), it is also called Wasserstein Distance. Informally, assuming there are two different piles of dirt $\mathbb{P}$ and $\mathbb{Q}$ with same total amount the EMD can be interpreted as the minimal cost for moving one distribution pile to another to make both $\mathbb{P}$ and $\mathbb{Q}$ have the same distribution. Thus we can calculate EMD as the sum of work for moving piles from $\mathbb{P}$ to $\mathbb{Q}$, for each move, the mass times the distance. Usually there are lots of ways for moving one distribution to another. Therefore to find the way with the minimal cost is an optimization problem.

Definition of discrete case:

$$\begin{aligned} W(\mathbb{P}_r, \mathbb{P}_g) &= \inf_{\gamma \in \Pi(\mathbb{P}_r, \mathbb{P}_g)} \sum_{\boldsymbol{x}, \boldsymbol{y}} \|\boldsymbol{x} - \boldsymbol{y}\| \gamma(\boldsymbol{x}, \boldsymbol{y}) \\ &= \inf_{\gamma \in \Pi(\mathbb{P}_r, \mathbb{P}_g)} \mathbb{E}_{(\boldsymbol{x}, \boldsymbol{y}) \sim \gamma} \big[\|\boldsymbol{x} - \boldsymbol{y}\|\big] \end{aligned} \tag{3.1}$$

where $\Pi(\mathbb{P}_r, \mathbb{P}_g)$ is the set of all combinations of joint distributions between $\mathbb{P}_r$ and $\mathbb{P}_g$. Since, γ means the percentage of earth should be moved from $\boldsymbol{x}$ to $\boldsymbol{y}$, thus $\mathbb{P}_g(\boldsymbol{y}) = \sum_{\boldsymbol{x}} \gamma(\boldsymbol{x}, \boldsymbol{y})$ and $\mathbb{P}_r(\boldsymbol{x}) = \sum_{\boldsymbol{y}} \gamma(\boldsymbol{x}, \boldsymbol{y})$, which means $\mathbb{P}_g(\boldsymbol{y})$ and $\mathbb{P}_r(\boldsymbol{x})$ are marginal distributions of $\gamma(\boldsymbol{x}, \boldsymbol{y})$ respectively.

Here is a simple example of how Earth Mover's Distance works, suppose X and Y are two different discrete random variables over the spaces $\mathbb{P}$ and $\mathbb{Q}$, then the EMD from $\mathbb{P}$ to $\mathbb{Q}$ is

$$\begin{aligned}\text{EMD}(\mathbb{P},\mathbb{Q}) =& 0.1 * |4-3| + 0.1 * |4-2| + 0.2 * |4-0| \\ &+ 0.2 * |5-1| + 0.3 * |6-2| + 0.1 * |7-3| \\ =& 3.5\end{aligned}$$

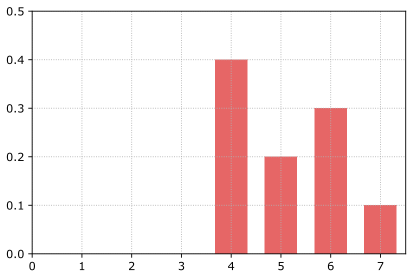
(a) Distribution of dirt $\mathbb{P}$

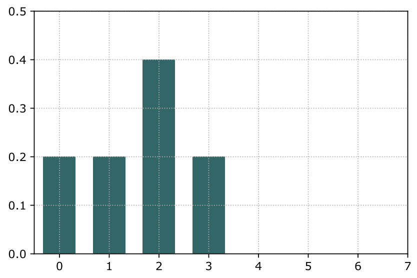
(b) Distribution of dirt $\mathbb{Q}$

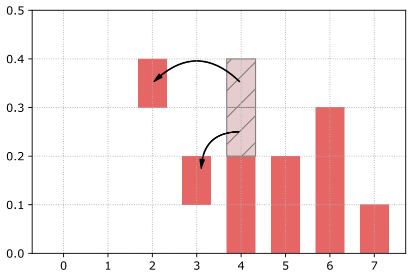
(c) Moving dirt $\mathbb{P}$ to $\mathbb{Q}$

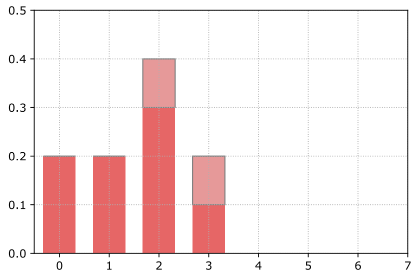
(d) transported $\mathbb{P}$

Figure 3.2: Transporting discrete probability distributions from $\mathbb{P}$ to $\mathbb{Q}$

3.2 Why is Wasserstain GAN better

Here is an example of why it is better to use Wasserstein distance (Example 1 from Arjovsky et al. 2017).

Let Y be the random variable $Y \sim U[0,1]$, $\mathbb{P}$ and $\mathbb{Q}$ are two probability distributions, where $\mathbb{P}$ is the distribution on $(0,Y) \in \mathbb{R}^2$, $\mathbb{Q}$ is $(\theta,Y) \in \mathbb{R}^2$ for $\theta \in [0,1]$. If $\theta \neq 0$ then we have:

$$
\begin{aligned}
KL(\mathbb{P}||\mathbb{Q}) &= \sum_{x=0, Y\sim U[0,1]} 1 \times \ln\frac{1}{0} = \infty \\
KL(\mathbb{Q}||\mathbb{P}) &= \sum_{x=\theta, Y\sim U[0,1]} 1 \times \ln\frac{1}{0} = \infty \\
JS(\mathbb{P}||\mathbb{Q}) &= \frac{1}{2}KL\Big(\mathbb{P}||\frac{\mathbb{P}+\mathbb{Q}}{2}\Big) + \frac{1}{2}KL\Big(\mathbb{Q}||\frac{\mathbb{Q}+\mathbb{P}}{2}\Big) \\
=&\frac{1}{2}\Big(\sum_{x=0, Y\sim U[0,1]} 1 \times \ln\frac{1}{0.5} + \sum_{x=\theta, Y\sim U[0,1]} 1 \times \ln\frac{1}{0.5}\Big) \\
=&\ln 2 \\
W(\mathbb{P},\mathbb{Q}) &= |\theta|
\end{aligned}
$$

If $\theta = 0$, then $\mathbb{P}$ and $\mathbb{Q}$ completely overlap. This indicates that in most cases, KL divergence is impossible to calculate when two distributions are discrete.

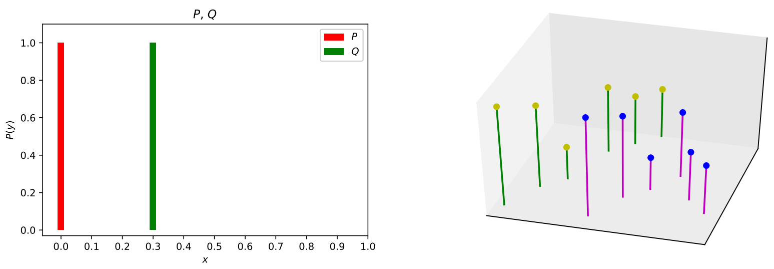

2d 3d

Figure 3.3: 2d and 3d plot of two non-overlapped discrete probability distributions $\mathbb{P}$ and $\mathbb{Q}$

The 3d plot just an example that when two distributions are completely non-overlapped in high dimensional space, the KL and Jensen Shannon divergence would be the same as the example showed by Arjovsky et al. (2017)

Assumption 3.1: [Assumption 1 (Arjovsky et al. 2017)]
Let $g : \mathcal{Z} \times \mathbb{R}^d \mapsto \mathcal{X}$ be locally Lipschitz between finite dimentional vector spaces, $g_\theta(z)$ is denoted as evaluation on corrdinates (z, θ). We call g satisfies assumption 1 for a certain probability distribution $\mathbb{P}$ over $\mathcal{Z}$ if there are local Lipschitz constants $K(\theta, z)$ such that:

$$\mathbb{E}_{z\sim\mathbb{P}}\big[K(\theta, z)\big] < \infty$$

Theorem 3.1: [Theorem 1 (Arjovsky et al. 2017)]

Let $\mathbb{P}_r$ be a fixed distribution over $\mathcal{X}$. Let Z be a random variable (e.g Gaussian) over another space $\mathcal{Z}$. Let $g : \mathcal{Z} \times \mathbb{R}^d \mapsto \mathcal{X}$ be a function, that will be denoted $g_\theta(\boldsymbol{z})$ with $\boldsymbol{z}$ the first coordinate and $\boldsymbol{\theta}$ the second. Let $\mathbb{P}_\theta$ denote the distribution of $g_\theta(Z)$. Then:

1. If g is continuous in $\boldsymbol{\theta}$, then $W(\mathbb{P}_r, \mathbb{P}_\theta)$ is also continuous.
2. If g is locally Lipschitz and satisfies regularity assumption 1, then $W(\mathbb{P}_r, \mathbb{P}_\theta)$ is continuous everywhere, and differentiable almost everywhere.

Proof.

Here is a summary of the proof by the original author:

1.

The goal is to show

$$\begin{aligned} &\lim_{\theta_1 \to \theta_2} \|g_{\theta_1}(\boldsymbol{z}) - g_{\theta_2}(\boldsymbol{z})\| = 0 \\ \implies &\lim_{\theta_1 \to \theta_2} \|W(\mathbb{P}_r, \mathbb{P}_{\theta_1}) - W(\mathbb{P}_r, \mathbb{P}_{\theta_2})\| = 0 \end{aligned}$$

Assume θ_1 and θ_2 are two parameter vectors in $\mathbb{R}^d$. By the definition of the Wasserstein distance,

$$\begin{aligned} W(\mathbb{P}_{\theta_1}, \mathbb{P}_{\theta_2}) &\leq \mathbb{E}_{(a,b)\sim\gamma}\left[\|x - y\|\right] \\ &= \mathbb{E}_{(a,b)\sim\gamma}\left[\|g_{\theta_1(z)} - g_{\theta_2(z)}\|\right] \\ &= \int_{\mathcal{X}\times\mathcal{X}} \left[\|g_{\theta_1(z)} - g_{\theta_2(z)}\|\right] d\gamma \end{aligned}$$

If g is continuous, by the property of continuity,

$$\begin{aligned} &\lim_{\theta_1 \to \theta_2} g_{\theta_1}(z) = g_{\theta_2}(z) \\ \implies &\|g_{\theta_1}(z) - g_{\theta_2}(z)\| = 0. \end{aligned}$$

Since we assumed that $\mathcal{X}$ is compact, which means closed and bounded, there exists a constant M such that $\|g_{\theta_1}(z) - g_{\theta_2}(z)\| \leq M$ uniformly for all $\theta \in \mathbb{R}^d$ and z. By the Lebesgue's dominated convergence theorem and (1),

$$\lim_{\theta_1 \to \theta_2} \int_{\mathcal{X}\times\mathcal{X}} \left[\|g_{\theta_1(z)} - g_{\theta_2(z)}\|\right] d\gamma = \lim_{\theta_1 \to \theta_2} \mathbb{E}_z\left[\|g_{\theta_1}(z) - g_{\theta_2}\|\right] = 0$$

by the triangle inequality:

$$\Big\|W\big(\mathbb{P}_r, \mathbb{P}_{\theta_1}\big) - W\big(\mathbb{P}_r, \mathbb{P}_{\theta_2}\big)\Big\| \leq W\big(\mathbb{P}_{\theta_1}, \mathbb{P}_{\theta_2}\big)$$

Therefore if $\theta_1 \to \theta_2$,

$$\lim_{\theta_1 \to \theta_2} W\big(\mathbb{P}_{\theta_1}, \mathbb{P}_{\theta_2}\big) = 0$$

The continuity of $W(\mathbb{P}_r, \mathbb{P}_\theta)$ is proved.
For proving 2, assumed g is Lipschitz locally, that is, for a given point (z, θ) in the domain of g, exists an open set $(z, \theta) \in U$ and a constant $K(z, \theta)$ such that $\forall (z', \theta') \in U$ satisfied the property,

$$\big\|g_\theta(z) - g_{\theta'}(z')\big\| \leq K(z,\theta)\big\|(\theta, z) - (\theta', z')\big\| \leq K(z,\theta)\big(\|\theta - \theta'\| + \|z - z'\|\big).$$

After taking expectation for both sides of the above equation and set $z = z'$,

$$\mathbb{E}_{z \sim \mathbb{P}_\theta}\big[\|g_\theta(z) - g_{\theta'}(z)\|\big] \leq \mathbb{E}_{z \sim \mathbb{P}_\theta}\big[K(z,\theta)\big]\big\|\theta - \theta'\big\| \qquad \forall\big(z, \theta'\big) \in U$$

define a new set

$$U_\theta := \big\{\theta' \big| (\theta', z) \in U\big\}.$$

Since U is open set, thus U_θ as well. Based on the above proof, by assumption 1 and define $K(\theta) = \mathbb{E}_{z \sim \mathbb{P}_\theta}\big[K(z,\theta)\big]$ we have:

$$\begin{aligned}\Big\|W\big(\mathbb{P}_r, \mathbb{P}_{\theta_1}\big) - W\big(\mathbb{P}_r, \mathbb{P}_{\theta_2}\big)\Big\| &\leq W\big(\mathbb{P}_{\theta_1}, \mathbb{P}_{\theta_2}\big)\\ &\leq \mathbb{E}_{z \sim \mathbb{P}_\theta}\big[\|g_\theta(z) - g_{\theta'}(z')\|\big]\\ &\leq K(\theta)\big\|\theta - \theta'\big\| \qquad \forall \theta' \in U_\theta\end{aligned}$$

this implies that $W\big(\mathbb{P}_r, \mathbb{P}_{\theta_1}\big)$ is locally Lipschitz, and also continuous everywhere. By Radamacher's theorem, $W\big(\mathbb{P}_r, \mathbb{P}_{\theta_1}\big)$ must be differentiable almost everywhere. $\square$

There is a corollary that guarantees that the Wasserstain Distance can be used as a loss function in neural networks.

Corollary 3.1: [Corollary 1 (Arjovsky et al. 2017)]

If g_θ is a feedforward neural network with $\boldsymbol{\theta}$ as it's parameters, that is, g_θ is a function composed by affine transformations and non-linear activation functions which are smooth Lipschitz continuous, and $\mathbb{E}_{z\sim p(z)}\big[\|z\|\big] < \infty$. Then the assumption 1 is satisfied and therefore $W(\mathbb{P}_r, \mathbb{P}_\theta)$ is continuous everywhere and differentiable almost everywhere.

3.3 Wasserstein GAN

The solution of Wasserstein distance' infimum form in (3.1) is hard to find. However, solving (3.1) is equivalent to solving the Kantorovich - Rubinstein duality (Villani. 2008)

$$W(\mathbb{P}_r, \mathbb{P}_\theta) = \sup_{\|f\|_L \leq 1} \mathbb{E}_{\boldsymbol{x}\sim\mathbb{P}_r(\boldsymbol{x})} - \mathbb{E}_{\boldsymbol{x}\sim\mathbb{P}_g(\boldsymbol{x})}$$

where all functions of $f : \mathcal{X} \mapsto \mathbb{R}$ are 1-Lipschitz. If we substitute $\|f\|_L \leq 1$ to $\|f\|_L \leq K$, then the left side of the above equations would be $K \cdot W(\mathbb{P}_r, \mathbb{P}_\theta)$, and we are still in the same optimization problem. Thus, we could solve the Wasserstein distance by maximizing

$$\max_{w\in\mathcal{W}} \mathbb{E}_{\boldsymbol{x}\sim\mathbb{P}_r(\boldsymbol{x})}\big[f_w(\boldsymbol{x})\big] - \mathbb{E}_{\boldsymbol{x}\sim\mathbb{P}_r(\boldsymbol{x})}\big[f_w(g(\boldsymbol{z}))\big]$$

Where w are parameters for a family of functions $\{f_w\}_{w\in\mathcal{W}}$, and w belong to a compact space $\mathcal{W}$, this implies that all f_w are K- Lipschitz functions depended only on $\mathcal{W}$. In order to implement that, Arjovsky et al. proposed to regulate all weights w of the discriminator's neural network, e.g., in their case, $w \in [-0.01, 0.01]$. However, Arjovsky et al. also pointed out that weight clipping is a bad way to implement the Lipschitz constraint. Since if the clipping bound is too large, it would make a lot of extra iterations for all weights w to converge to their limit. On the contrary, if the clipping bound is too small, it would cause vanishing gradients. But still, since the Wasserstein distance is differentiable almost everywhere, ideally, the critic could be trained until optimization.

In addition, the backpropagation of G is described in the theorem below

Theorem 3.3: [Theorem 3 (Arjovsky et al. 2017)]
Assume $\mathbb{P}_r$ is a distribution, and $\mathbb{P}_g$ is another distribution over $g_\theta(Z)$ with Z as random variable, and $g_\theta(Z)$ satisfies assumption 1, then there exists a solution $f : \mathcal{X} \mapsto \mathbb{R}$ for (5). Moreover,

$$\nabla_\theta W(\mathbb{P}_r, \mathbb{P}_\theta) = -\mathbb{E}_{\boldsymbol{z}\sim p_g(z)}\big[\nabla_\theta f(g_\theta(\boldsymbol{z})\big].$$

With the theory that is explained above, we have that the final WGAN algorithm they developed is like below

Algorithm 2: WGAN algorithm with default hyperparameters proposed by Arjovsky et al. Both D and G are using RMSprop as optimizer, with learning rate $\lambda = 0.00005$, weight clip c = 0.01, $n = 5$, batch size $k = 64$

```
1: while before $\theta$ converged do
2:     for training discriminator $n$ iterations do
3:         Sample $k$ minibatch random noise from latent space distribution $p_g(\boldsymbol{z})$
4:         Sample $k$ minibatch input examples from data distribution $p_r(\boldsymbol{x})$
5:         Backpropagating all weights in $D$ by maximizing and updating the loss:
               $$g_{w_D} \leftarrow \nabla_{w_D} \frac{1}{k} \sum_{i=1}^{k} \Big[ f_w(\boldsymbol{x}^{(i)}) - f_w\big(g(\boldsymbol{z}^{(i)})\big) \Big].$$
6:         $w_D \leftarrow w_D + \lambda \cdot$ RMSProp($w_D, g_{w_D}$)
7:         $w_D \leftarrow$ clip($w_D, [-c, c]$) $\forall w_D \notin [-c, c]$
8:     end for
9:     Sample $k$ minibatch random noise from latent space distribution $p_g(\boldsymbol{z})$
10:    Backpropagating all weights in $G$ by maximizing and updating the loss:
               $$g_{W_G} \leftarrow -\nabla_{W_G} \frac{1}{k} \sum_{i=1}^{k} \Big[ f_w\big(g(\boldsymbol{z}^{(i)})\big) \Big]$$
11:    $w_G \leftarrow w_G - \lambda \cdot$ RMSProp($w_G, g_{w_G}$)
12: end while
```

The loss function is an approximation of the Wasserstain distance.

Chapter 4

Two improved WGANs

Since Wasserstein GAN still not perfect, there are researchers analyzed it's faults and tried to fixed them.

4.1 Wasserstein GAN with Gradient Penalty (WGAN-GP)

In the previous chapter, we saw that in Wasserstein GAN, Arjovsky et al introduced the new loss functions for D and G respectively

- $L(D) = -\mathbb{E}_{\boldsymbol{x}\sim p_r(\boldsymbol{x})}\big[D(\boldsymbol{x})\big] + \mathbb{E}_{\boldsymbol{x}\sim p_g(\boldsymbol{z})}\big[D(G(\boldsymbol{z}))\big]$
- $L(G) = \mathbb{E}_{\boldsymbol{x}\sim p_g(\boldsymbol{z})}\big[D(G(\boldsymbol{z}))\big]$

By the Kantorovich-Rubinstein duality, the weight clipping enforces a K-Lipschitz constraint. In other words, the L2 norm of D's gradient must be bounded by a constant K

$$\big\|\nabla_{\boldsymbol{x}} D(\boldsymbol{x})\big\| \leq K$$

In the previous chapter, Arjovsky et al introduced weight clipping

$$w \leftarrow \text{clip}(w, [-c, c])$$

to implement Lipschitz constrain, where c is the hyperparameter. However, as Gulrajani et al pointed out in their paper, this method has two problems:

1. The gradient can easily vanish or explode
2. Most of the weights are distributed on the clipping boundary, i.e., either equals to $-c$ or c.

In the first problem, since discriminators usually are deep neural networks, by the chain rule, if the clipping of the constant c is being set relatively small the backpropagation can cause the gradient to vanish; if c were set relatively big, the gradient can easily explode. Instead of applying weight clipping, Gulrajani et al showed that on the Swiss Roll dataset (Figure 10) the gradient penalty term can make the gradient stable through each layer.

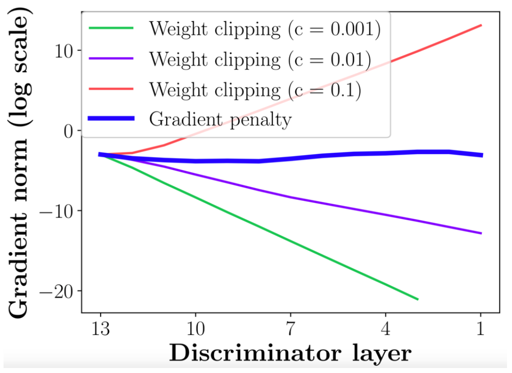

Figure 10: x axis indicate layer's index . Figure 1(b) in Gulrajani et al [17]

In the second problem, the weights are bounded on a interval $[-c, c]$, i.e., allthose weights greater than c will be set to c, all those less than $-c$ will set back to $-c$. This would cause the discriminator to learn a simple function. Gulrajani et al verified the problem on the Swiss Roll dataset and found that most of the weights take either the value c or $-c$. Instead, the gradient penalty term does not suffer from this issue, Figure 11 demonstrates this.

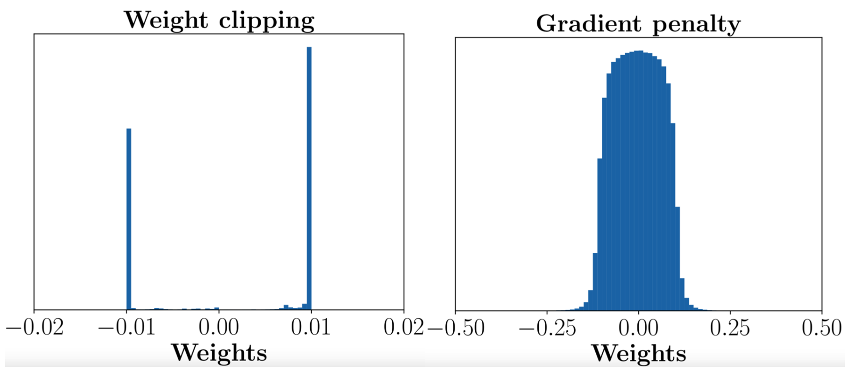

(a) (b)

Figure 11: Figure 1(b) from Gulrajani et al [17]

The above two problems indicate that for the weight clipping method, model performance is too sensitive with respect to the corresponding hypermarameter c.

A differentiable function is K-Lipschitz if and only if the Euclidean norm of it's gradient is almost K everywhere. Instead of using weight clip, Gulrajani et al proposed to add a gradient penalty term which, as mentioned above, enforces 1-Lipschitz constraint.

$$\left(\left\|\nabla_{\boldsymbol{x}} D(\boldsymbol{x})\right\| - 1\right)^2$$

with the discriminator sufficiently trained, the norm of it's gradient will converge to 1. Then the new loss function to be minimized becomes

$$L = \underbrace{\mathbb{E}_{\boldsymbol{z}\sim\mathbb{P}_g}\big[D(g(\boldsymbol{z})\big] - \mathbb{E}_{\boldsymbol{x}\sim\mathbb{P}_r}\big[D(\boldsymbol{x})\big]}_{\text{original WGAN's loss}} + \underbrace{\lambda \cdot \mathbb{E}_{\hat{\boldsymbol{x}}\sim\mathbb{P}_{\hat{\boldsymbol{x}}}}\Big[\big(\|\nabla_{\hat{\boldsymbol{x}}} D(\hat{\boldsymbol{x}})\|_2 - 1\big)^2\Big]}_{\text{new gradient penalty term}}.$$

Where $\hat{\boldsymbol{x}} = \epsilon\boldsymbol{x} + (1-\epsilon)g(\boldsymbol{z})$ and ϵ is a random real number from [0,1]. Thus any model can be penalized by the gradient penalty term if the norm of the gradient diverges from 1.

For experiment setting, Gulrajani et al proposed to not use batch normalization, but layer normalization is recommended. Below is the final algorithm:

Algorithm 3: [Algorithm 1 in Gulrajani et al [17]]. The default hyperparameters are $\lambda = 10, n = 5, \beta_1 = 0, \beta_2 = 0.9, \alpha = 0.0001$, where β_1, β_2 and α are Adam optimizer hyperparameters

```
1: while before $\theta$ converged do
2:     for training discriminator $n$ iterations do
3:         for $i = 1, \cdots,$ batch size $m$ do
4:             Sample $\boldsymbol{x}$ from data distribution $p_r(\boldsymbol{x})$
5:             Sample $\boldsymbol{z}$ from latent space $p_g(\boldsymbol{z})$
6:             Sample random number $\epsilon$ from $U[0,1]$
7:             $\hat{\boldsymbol{x}} \leftarrow \epsilon\boldsymbol{x} + (1-\epsilon)G_\theta(\boldsymbol{x})$
8:             $L^{(i)} \leftarrow D\big(G(\boldsymbol{z})\big) - D(\boldsymbol{z}) + \lambda\big(\|\nabla_{\hat{\boldsymbol{x}}} D(\hat{\boldsymbol{x}})\|_2 - 1\big)^2$
9:         end for
10:        $w_D \leftarrow w_D - \eta\cdot$ Adam$\Big(\frac{1}{m}\sum_{i=1}^m \nabla_{w_D} L^{(i)}, \beta_1, \beta_2, \alpha\Big)$
11:    end for
12:    Sample $k$ minibatch random noise from latent space distribution $p_g(\boldsymbol{z})$
11:    $w_G \leftarrow w_G - \eta\cdot$ Adam$\Big(-\frac{1}{m}\sum_{i=1}^m \nabla_{w_G} D\big(G(\boldsymbol{z}^{(\boldsymbol{i})}), \beta_1, \beta_2, \alpha\big)\Big)$
12: end while
```

4.2 Wasserstein GAN with A Consistency Term (CT-GAN)

Despite the fact that WGAN with gradient penalty term is able to overcome the two problems which exist in the original WGAN, Wei et al. (2017) indicate that the gradient penalty term can not penalize all sample points, only works on those interpolated samples $\hat{\boldsymbol{x}}$. Moreover, at the early training stages, the distribution $\mathbb{P}_g$ differs a lot from $\mathbb{P}_r$, and makes the Lipschitz continuity fail to be constrained until $\mathbb{P}_r$ and $\mathbb{P}_g$ close to each other.

Based on these issues, they attempt to improve the WGAN with gradient penalty by enforcing the Lipschitz continuity over the real data $\boldsymbol{x} \sim \mathbb{P}_r$. Specifically, they perturb each real sample $\boldsymbol{x}$ as $\boldsymbol{x}'$ and $\boldsymbol{x}''$, then apply Lipschitz constraint to bound the $D(\boldsymbol{x}')$ and $D(\boldsymbol{x}'')$.

Recall from the WGAN with gradient penalty, a discriminator $D : \mathcal{X} \mapsto \mathcal{Y}$ is Liptschitz continuous if and only if there exists a real number K such that $\forall \boldsymbol{x}_1, \boldsymbol{x}_2 \in \mathcal{X}$,

$$\|D(\boldsymbol{x}_1) - D(\boldsymbol{x}_2)\|_2 \leq K \cdot \|\boldsymbol{x}_1 - \boldsymbol{x}_2\|_2$$

therefore, the following soft consistency term (CT) can be added in order to penalize those violations from the above inequality.

$$CT\big|_{\boldsymbol{x}_1,\boldsymbol{x}_2} = \mathbb{E}_{\boldsymbol{x}_1,\boldsymbol{x}_2}\Big[\max\Big(\frac{\|D(\boldsymbol{x}_1) - D(\boldsymbol{x}_2)\|_2}{\|\boldsymbol{x}_1 - \boldsymbol{x}_2\|_2} - M', 0\Big)\Big]$$

However, Wei et al pointed out that $\|\boldsymbol{x}_1 - \boldsymbol{x}_2\|$ is impractical, as it is hard to compute all the combinations of $\|\boldsymbol{x}_i - \boldsymbol{x}_j\|$, where $i, j \in \mathbb{N}^+$. Therefore, to make the inequality able to be implemented, all $\|\boldsymbol{x}_i - \boldsymbol{x}_i\|_2$ are assumed to be bounded by a constant M', and M' is a hyper-parameter, the best results which they found are in the range [0, 0.2]. In addition, they proposed to apply dropout before the output of the discriminator, denoted as $D(\boldsymbol{x}')$, where $\boldsymbol{x}'$ is sampled from input data, and $D(\boldsymbol{x}'')$ is the second data point which is applied in the same corresponding way. $D\_(\cdot)$ denote the output of the second last layer of the discriminator. Thus the final consistency term and loss function they developed are

$$CT\big|_{\boldsymbol{x}',\boldsymbol{x}''} = \mathbb{E}_{\boldsymbol{x}\sim\mathbb{P}_r}\big[\max\big(0, \|D(\boldsymbol{x}_1) - D(\boldsymbol{x}_2)\|_2\big) + 0.1\big(\|D\_(\boldsymbol{x}') - D\_(\boldsymbol{x}'')\|_2 - M'\big)\big],$$

$$L = \mathbb{E}_{\boldsymbol{z}\sim\mathbb{P}_g}\big[D(G(\boldsymbol{z}))\big] - \mathbb{E}_{\boldsymbol{x}\sim\mathbb{P}_r}\big[D(\boldsymbol{x})\big] + \lambda_1 GP\big|_{\hat{\boldsymbol{x}}} + \lambda_2 CT\big|_{\boldsymbol{x}',\boldsymbol{x}''},$$

and the final algorithm for the CT-GAN is

Algorithm 4: [Algorithm 1 in Wei et al [14]]. The default hyperparameters are $\lambda_1 = 10, \lambda_2 = 2, n = 5, \beta_1 = 0.5, \beta_2 = 0.9, \alpha = 0.0002, m = 64$ where β_1, β_2 and α are Adam optimizer hyperparameters.

```
1: while before $\theta$ converged do
2:     for training discriminator $n$ iterations do
3:         for $i = 1, \cdots$, batch size $m$ do
4:             Sample $\boldsymbol{x}$ from data distribution $p_r(\boldsymbol{x})$
5:             Sample $\boldsymbol{z}$ from latent space $p_g(\boldsymbol{z})$
6:             Sample random number $\epsilon$ from $U[0,1]$
7:             $\hat{\boldsymbol{x}} \leftarrow \epsilon\boldsymbol{x} + (1-\epsilon)G_\theta(\boldsymbol{x})$
8:             $L^{(i)} \leftarrow D\big(G(\boldsymbol{z})\big) - D(\boldsymbol{z}) + \lambda_1 GP\big|_{\hat{\boldsymbol{x}}} + \lambda_2 CT\big|_{\boldsymbol{x}',\boldsymbol{x}''}$
9:         end for
10:        $w_D \leftarrow w_D - \eta\cdot$ Adam $\Big(\frac{1}{m}\sum_{i=1}^m \nabla_{w_D} L^{(i)}, \beta_1, \beta_2, \alpha\Big)$
11:    end for
12:    Sample $k$ minibatch random noise from latent space distribution $p_g(\boldsymbol{z})$
11:    $w_G \leftarrow w_G - \eta\cdot$ Adam$\Big(-\frac{1}{m}\sum_{i=1}^m \nabla_{w_G} D\big(G(\boldsymbol{z}^{(i)}), \beta_1, \beta_2, \alpha\Big)$
12: end while
```

Chapter 5

Experiments

Conneau et al showed results trained by Vanilla GAN for some language pairs such as English(en) translated to Spanish(es), English to French(fr) and English to Esperanto(eo) etc. Their code, dictionaries and word embeddings are open source on GitHub (MUSE)[1].

Since the GPU computational resource is limited, and for the convenience of comparing the result and baseline from the MUSE, we only select several relatively representative language pairs which Conneau et al. (2017) implemented, and plus few other language pairs.

We will describe the data we used and review the experimental procedure in details from Conneau et al first, then show our result.

5.1 data description

Facebook's AI Research department published pre-trained word vectors for 294 languages in GitHub. They trained them on Wikipedia as source text using the library called fastText. More specifically, the word vectors were trained using the skip-gram models (Bojanowski et al. 2016) with 300 as embedding dimension. All datasets can be downloaded from their GitHub repository [2].

We also tried to fit English embeddings which are trained from different corpus, plus by Global Vectors (Pennington et al. 2014), which is another word representation algorithm. The source corpus of this English embeddings are trained from English Common Crawl Corpus (ENC3) [3], which contains two million word embeddings.

5.2 Multilingual Unsupervised and Supervised Embeddings

In the unsupervised method of MUSE, they assumed that any given two monolingual word embeddings are isomorphic, and the linear transformation W

[1] MUSE: Multilingual Unsupervised and Supervised Embeddings
[2] FastText: Pre-trained word vectors
[3] NLPL word embeddings repository

across source language embeddings to target embeddings can be learned by GANs without any given dictionary. The experimental setup will be reviewed in this section.

5.2.1 Network architecture

Based on the assumption, Conneau et al. (2018) defined the generator as a linear transformation W which maps the source embedding matrix X to the target embedding matrix Y, therefore the generator is a single-layer neural network without activation function, the number of nodes in that layer depends on the embedding dimension of language pairs. Since the dimensionality of all monolingual embeddings in MUSE is 300, hence the generator is a square matrix with size 300×300.

The discriminator is a multilayer perceptron with two hidden layers, both have 2048 nodes with Leaky-ReLu as activation function, plus 0.1 dropout noise to the discriminator's input. The output of the discriminator is a value of probability.

5.2.2 Objective functions

Assume $\mathcal{X} = \{\boldsymbol{x}^{(1)}, \cdots, \boldsymbol{x}^{(n)}\}$ and $\mathcal{Y} = \{\boldsymbol{y}^{(1)}, \cdots, \boldsymbol{y}^{(m)}\}$ are source and target language embeddings respectively, the label for source embedding is 1, 0 for target. Since the goal of the discriminator is to identify whether the input is coming from source or target. Therefore the discriminator's loss function is

$$f\mathcal{L}_D = -\frac{1}{n}\sum_{i=1}^{n} \log P_{\theta_D}\left(\text{source} = 1 \middle| W\boldsymbol{x}^{(i)}\right) - \frac{1}{m}\sum_{i=1}^{n} \log P_{\theta_D}\left(\text{target} = 0 \middle| \boldsymbol{y}^{(i)}\right)$$

where θ_D denote the parameters of discriminator's network, $P_{\theta_D}\left(\text{source} = 1 \middle| W\boldsymbol{x}\right)$ means probability of input point coming from source embeddings, whereas $P_{\theta_D}\left(\text{target} = 0 \middle| \boldsymbol{y}\right)$ means target embeddings, i.e., real dataset.

The task of the generator is to deceive the discriminator as much as possible, thus, it's loss function is

$$\mathcal{L}_W = -\frac{1}{n}\sum_{i=1}^{n} \log P_{\theta_D}\left(\text{source} = 0 \middle| W\boldsymbol{x}^{(i)}\right) - \frac{1}{m}\sum_{i=1}^{n} \log P_{\theta_D}\left(\text{target} = 1 \middle| \boldsymbol{y}^{(i)}\right)$$

5.2.3 Optimizer

Since they use minibatch for each training iteration and the batch size is 32, stochastic gradient descent is applied for minimizing $\mathcal{L}_D$ and $\mathcal{L}_W$, the default learning rate is 0.1 without momentum.

5.2.4 Orthogonality

Since the generator is a 300×300 matrix, Conneau et al. (2018) proposed to apply an orthogonal constraint to the generator after each minibatch iteration. It keeps the embeddings' quality after the source embedding is translated. Moreover, orthogonal matrices have a nice property, assuming $\mathcal{O}$ is an orthogonal matrix, i.e. $\mathcal{O}^T\mathcal{O} = \mathcal{O}\mathcal{O}^T = I$, it will preserve the ℓ_2 norm,

$$\|\mathcal{O}\boldsymbol{x}\|_2^2 = \langle \mathcal{O}\boldsymbol{x}, \mathcal{O}\boldsymbol{x}\rangle = \mathcal{O}^2\langle \boldsymbol{x}, \boldsymbol{x}\rangle = \|\boldsymbol{x}\|_2^2$$

This implies $\|\mathcal{O}\boldsymbol{x}\|_2 = \|\boldsymbol{x}\|_2$, in addition this means $\mathcal{O}$ is an isometry in the $\ell 2$ space because it preserves distance.

The algorithm they used to update the transformation W is

$$W \longleftarrow (1+\beta)W - \beta(WW^T)W$$

where β is a hyperparameter, as they suggest, $\beta = 0.01$ performs well.

5.2.5 Cross-domain similarity local scaling (CSLS)

A reliable metric is crucial for the criterion of model selection, as we need to compare the similarity between source embeddings and target embeddings.

Nearest neighbors have the asymmetric property, which means that if x is the k-nn of a point y, it does not imply that y is a k-nn of x. By Radovanović et al. (2010), the asymmetric property would cause harmful results in high dimensional spaces: some points, which are called hubs, are the nearest neighbors of numerous other points, however, for some other points, which are called anti-hubs, there are no points having them as the nearest neighbors.

Therefore, Conneau et al. (2018) proposed a bi-partite neighborhood graph called Cross-domain similarity local scaling(CSLS) as the new metric. By their definition, the mean cosine similarity from a translated source embedding Wx_s to its k-target neighborhood in target space is defined as

$$r_T(Wx_s) = \frac{1}{k}\sum_{y_t \in \mathcal{N}_T(Wx_s)} \cos(Wx_s, y_t)$$

where $\mathcal{N}_T(Wx_s)$ denotes the neighborhood associated with a translated source word Wx_s, and all k words of $\mathcal{N}_T(Wx_s)$ are from target embeddings. Similarly, $\mathcal{N}_S(y_t)$ denote the neighborhood in target embedding corresponded to a target word y_t. The mean cosine similarity of a target word to its k-target neighborhood in translated source embeddings space is defined as

$$r_S(y_t) = \frac{1}{k}\sum_{Wx_s \in \mathcal{N}_S(y_t)} \cos(y_t, Wx_s)$$

these two mean cosine scores for translated source embeddings and target embeddings are implemented by the library called Faiss[4], which greatly speed up the computation of nearest neighbors. The Faiss is developed by Johnson et al. (2017) who are members of Facebook AI research group. The CSLS algorithm define as

$$\text{CSLS}(Wx_s, y_t) = 2\cos(Wx_s, y_t) - r_T(Wx_s) - r_S(y_t).$$

[4]Faiss: a package for efficient similarity computation.

Obviously, there is no hyperparameter tuning requirement for it. By the interpretation of Conneau et al. (2018) , the update of CSLS algorithm increases the similarity for those anti-hub word embeddings. In contrast, it also reduces those embeddings in dense hub regions. In addition, the CSLS greatly improves the translation accuracy in experiments.

5.2.6 Translation process

The MUSE will translate source embeddings to the target embedding space, then for each translated source embedding, select the k-nearest neighbors from target embeddings, by CSLS algorithm.

5.2.7 Evaluation procedure

Conneau et al provides some bilingual evaluation dictionaries which are translated by an internal translation tool, each dictionary translate 1500 unique source words, most of them are commonly used, also polysemy for some vocabularies, i.e., the English word "discover" translated to the Spanish words : "descubrir", "descubra", "descubre" and "descubren". After each epoch, the MUSE will calculate the CSLS accuracy on bilingual evaluation dictionary, and report the precision at 1(P@1), 5(P@5) and 10(P@10).

MUSE will also compute the similarity for the top 10,000 frequent words. After having finished the calculation of CSLS precision, the length of both source and target embeddings will be normalized to 1, then a subset of source word index which corresponds to the temporary dictionary will be selected (source and target word embeddings would be indexed as temporary dictionary before adversarial training), and transformed by the learned generator, to match the target word by k-nearest neighbor and CSLS algorithm. At the end of the epoch, the best model will be saved based on the mean cosine CSLS for the maximum of 10,000 top frequent embeddings.

5.2.8 Procruster refinement

To improve the quality of W, they use the most frequent words as anchor points, then apply the Procruster algorithm, i.e., compute the SVD(YX^T), where X and Y are source and target embeddings respectively, then use U and V to solve

$$W^* = \underset{W}{\text{argmin}} \, \|WX - Y\|_F = UV^T,$$

they said that the refinement procedure slightly improved the performance.

5.3 Experimental set up

In our experiment, we focused on three improved GANs, i.e., Wasserstain GAN, WGAN with gradient penalty and CT-GAN. Our code is based on MUSE, in which we are using Pytorch as deep learning library instead of TensorFlow. We also found that adding layer normalization to the discriminator's hidden layers not only increases the accuracy, but also stabilizes the training process. Therefore, we will later show the results of all the three lineages of WGANs with layer normalization. Moreover, we are only focusing on the results obtained from adversarial training instead of after Procruster refinement.

5.3.1 Target language selection

We fixed English as the source language, and selected all the other languages from the table 2 of Søgaard et al (2018) as target languages, which are Spanish(ES), Estonian(ET), Greek(EL), Finnish(FI), Hungary(HU) and Polish(PL), plus Chinese(ZH), which belong to a different language family, and English whose embeddings are trained from a different corpus.

5.3.2 Network architecture

We keep using the same network architecture for all three improved GANs, i.e., two hidden layers with 2048 dimensionality, but, different loss functions. Plus added layer normalization to each of discriminator's hidden layers.

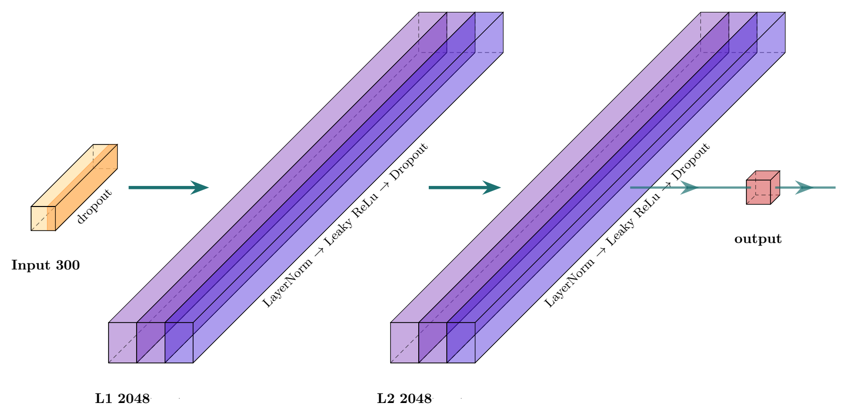
dropout
Input 300
LayerNorm → Leaky ReLu → Dropout
L1 2048
LayerNorm → Leaky ReLu → Dropout
L2 2048
output

Figure 5.1: Architecture of discriminator

In the above figure, each big purple block representing one hidden layer, and the sub-blocks means the states of them, e.g, for the first hidden layer, it is normalized by layer normalization at beginning, then transformed by Leaky Relu. Note, only the CT-GAN have 0.1 dropout on the two hidden layers, but not the WGAN and WGAN with gradient penalty.

5.3.3 Define the metric

There are two metrics which mentioned at the previous section can be used to select models and hyper-parameters.

- The CSLS nearest neighbor precision at 1, 5 and 10, which evaluate the performance on the evaluation dictionary.

- The mean cosine CSLS, which measure the similarity of the top frequent 10,000 words.

In table 5.1, the source language is English, we can see that the mean cosine CSLS inaccurately reflect translation performance, e.g. for English translate to Chinese(ZH) and Estonian(ET), the precision 10 of ET is very low and ZH is 0, but both of the tasks have high overall mean CSLS, this indicates that the translated embeddings have very close neighbors, but almost all of them are incorrect translations. Therefore, we use CSLS at P@1, 5 and 10 to evaluate translation performance.

Vanilla	**en**	**es**	**et**	**el**	**fi**	**hu**	**tr**	**pl**	**zh**
p@1	0.0	39.8	3.2	13.9	10.3	19.1	16.4	20.3	0.0
p@5	0.0	67.8	9.8	28.4	26.3	38.6	31.8	46.5	0.0
p@10	0.0	75.1	14.2	36.4	35.8	48.1	39.9	57.4	0.0
mean csls	47.9	67.1	49.6	56	56.1	56.8	55.5	58.6	79.6

Table 5.1: p@5, p@10 and mean cosine CSLS for differen target languages

5.3.4 Hyper-parameter search

Since the hyper-parameter search costs lot of GPU resources, we decide to only tune those main hyper-parameters which mostly affect our models. For those secondary hyper-parameters such as β_1 and β_2 in Adam optimizer, we are using the default values from PyTorch. We also found that instead of exponentially shrinking the learning rate for each epochs, fixed the learning rates until the training process finished performs better.

We first used grid search to find relatively good hyper-parameters from English to Spanish for all three different Algorithms, then extend to other languages pairs. The optimal hyper-parameters shown below:

- For WGAN, $c = 0.25$, lr$= 0.0005$ with RMSprop optimizer
- For WGAN with gradient penalty, $\lambda = 0.5$, lr$= 0.0005$ with Adam optimizer.
- For CT-GAN, $\lambda_{GP} = 0.5, \lambda_{CT} = 2$ and $M' = 0.2$, lr$= 0.0005$ with Adam optimizer.

The discriminator and generator shape the same settings of optimizers.

5.3.5 Stability test

Since the performance depends on how the weights are initialized, e.g., an experiment can produce a good result, but in the same setting with different random weight initialization, the generator may fail. Therefore, for all algorithms, we fixed hyper-parameters and let ten different random seeds vary, to test how stable these WGANs are. In addition, we defined a run as failed if the corresponding P@10 is less than 10%.

5.3.6 Baseline

We tried to reproduce the result in table 1 of Conneau et al , but we could not get the same result. This may be due to the best random seed not being specified, hence we implement the same setting from their paper, and use the new reproduced results as our baseline.

5.4 Results

We will first show the best results which we found with random seed -1 which is the one we were using for hyper-parameter search, them report the ten-run which with different random seeds later. All of our accuracy results are shown in percentage.

Vanilla	**en**	**es**	**et**	**el**	**fi**	**hu**	**tr**	**pl**	**zh**
p@1	0.0	39.8	3.2	13.9	10.3	19.1	16.4	20.3	0.0
p@5	0.0	67.8	9.8	28.4	26.3	38.6	31.8	46.5	0.0
p@10	0.0	75.1	14.2	36.4	35.8	48.1	39.9	57.4	0.0
WGAN	**en**	**es**	**et**	**el**	**fi**	**hu**	**tr**	**pl**	**zh**
p@1	0.0	40.4	1	7.7	4.1	16.5	0.0	0.0	0.0
p@5	0.1	68.6	3.5	19.2	12.4	34.8	0.0	0.0	0.1
p@10	0.1	75.6	6.2	26.5	17	43.5	0.1	0.1	0.1
WGAN-GP	**en**	**es**	**et**	**el**	**fi**	**hu**	**tr**	**pl**	**zh**
p@1	83.7	36.3	11.2	13.2	14.5	23	16.2	19.6	5.7
p@5	89.3	64.3	24.2	29.5	34.3	44	31.1	43.8	12.6
p@10	90.8	71.3	30.9	36.6	42.3	52.5	38.5	53.8	16
CT-GAN	**en**	**es**	**et**	**el**	**fi**	**hu**	**tr**	**pl**	**zh**
p@1	74.0	27.2	6.0	8.4	11.1	16.5	10.3	13.8	0.2
p@5	80.7	50.8	14.9	20.9	25.7	34	24.2	34.6	1.1
p@10	82.4	58.5	19.6	28.0	32.9	41.9	30.5	43.8	1.8

Table 5.2: p@1 and p@5, p@10 , random seed is -1

As we can from the above table, WGAN with gradient penalty(WGAN-GP) works best, and outperform the result did by Vanilla GAN. WGAN acquired worst result among all the four. Moreover, the performance of CT-GAN is quite close to Vanilla GAN.

5.4.1 stability test

We changed ten different random seeds for all the four algorithms, in order to test how weight initialization influence the training process.

Vanilla	**en**	**es**	**et**	**el**	**fi**	**hu**	**tr**	**pl**	**zh**
Failed	10	1	9	0	0	1	1	0	10
max p@1	0.1	39.6	5.7	13.7	13.5	25.6	17.2	24.9	0.0
min p@1	0.0	37.9	0.0	12.0	9.1	21.5	10.9	17.3	0.0
avg p@1	0.0	39.2	0.6	12.2	11.1	22.7	15.0	19.5	0.0
std p@1	0.0	0.7	1.7	1.0	1.6	1.2	2.1	2.6	0.0
max p@5	0.1	67.7	15.6	30.0	31.7	45.2	34.0	50.7	0.1
min p@5	0.1	63.8	0	25.1	23.4	39.6	24.5	40.1	0.0
avg p@5	0.1	66.8	1.6	27.4	27.5	42.4	30.1	43.4	0.0
std p@5	0.0	1.2	4.7	1.8	2.5	1.6	3.1	3.4	0.0
max p@10	0.4	74.9	22.4	37.7	65.7	54.5	0.103	61.0	0.1
min p@10	0.1	71.4	0	31.8	31.3	47.5	30.9	50.3	0.0
avg p@10	0.1	74.1	2.3	34.8	35.5	51.3	37.5	53.8	0.1
std p@10	0.1	1.1	6.7	2.0	2.9	1.8	3.7	3.5	0.0

Table 5.3: result of ten-run Vanilla GAN with differen random seed

WGAN	**en**	**es**	**et**	**el**	**fi**	**hu**	**tr**	**pl**	**zh**
Failed	10	2	9	10	10	4	5	4	8
max p@1	0.0	38.7	6.0	0.5	1.5	20.4	8.9	17.7	6.1
min p@1	0.0	0.0	0.0	0.0	0.0	0.0	0.0	0.0	0.1
avg p@1	0.0	30.4	0.9	0.1	0.2	9.1	3.5	8.8	1.2
std p@1	0.0	15.2	1.9	0.2	0.4	7.9	3.5	7.4	2.4
max p@5	0.1	65.4	14.7	1.2	5.1	22.0	20.9	39.1	13.6
min p@5	0.0	0.0	0.0	0.0	0.0	0.0	0.0	0.0	0.1
avg p@5	0.0	52.1	2.2	0.3	0.8	16.5	9.0	20.5	2.7
std p@5	0.0	26.0	4.6	0.3	1.5	8.3	8.8	17.0	5.3
max p@10	0.1	73.0	21.0	2.2	8.0	29.1	28.7	49.1	18.5
min p@10	0.0	0.1	0.1	0.0	0.0	0.0	0.0	0.0	0.1
avg p@10	0.0	58.0	3.2	0.5	1.3	22.1	12.3	26.3	3.7
std p@10	0.0	28.9	6.6	0.6	2.3	11.1	11.9	21.6	7.1

Table 5.4: result of ten-run WGAN original for different random seed

WGAN-GP	**en**	**es**	**et**	**el**	**fi**	**hu**	**tr**	**pl**	**zh**
Failed	1	0	0	0	0	1	0	0	0
max p@1	86.9	35.5	11.0	14.2	16.0	23.7	15.4	18.6	6.9
min p@1	0.0	34.6	10.3	6.7	13.4	0.0	11.9	16.2	3.4
avg p@1	76.3	35.0	9.9	8.6	14.5	19.7	14.7	17.8	5.3
std p@1	25.6	0.4	1.1	2.0	1.0	6.7	1.4	0.7	1.2
max p@5	91.8	62.2	24.0	31.0	36.0	44.9	32.6	43.8	14.2
min p@5	0.1	59.7	21.0	17.9	31.5	0	27.4	40.9	9.1
avg p@5	80.9	61.3	22.5	20.7	33.6	38.1	30.6	42.6	11.9
std p@5	27.0	0.8	1.2	3.6	1.4	12.8	1.7	0.9	1.9
max p@10	93.6	69.7	31.7	38.3	44.5	53.5	40.9	54.5	18.6
min p@10	0.4	67.5	27.0	23.3	39.5	0.1	35.6	50.9	12.0
avg p@10	82.1	68.7	29.1	26.9	42.1	45.8	38.3	52.7	15.3
std p@10	27.3	0.6	1.3	4.0	1.5	15.3	1.5	1.2	2.1

Table 5.5:WGAN-GP with ten-run different random seed

CT-GAN	**en**	**es**	**et**	**el**	**fi**	**hu**	**tr**	**pl**	**zh**
Failed	7	0	0	0	1	0	0	0	10
max p@1	71.9	32.1	5.8	10.5	10.9	15.7	10.8	13.7	0.1
min p@1	0.0	28.8	4.2	8.3	0.0	13.4	8.9	12.5	0.0
avg p@1	21.9	30.3	5.2	9.2	9.1	15.3	9.4	13.3	0.0
std p@1	32.8	1.2	0.7	1.1	3.1	0.9	0.9	0.5	0.0
max p@5	80.7	54.8	15.7	23.9	26.9	34.8	23.8	34.2	0.4
min p@5	0.0	51.3	12.5	19.2	0.1	30.4	20.2	30.5	0.0
avg p@5	24.7	53.3	13.9	21.8	22.2	33.2	22.0	32.6	0.2
std p@5	36.2	1.3	1.1	1.8	7.5	1.4	1.2	1.1	0.1
max p@10	83.2	63.0	22.0	30.4	35.6	44.6	30.5	44.0	0.7
min p@10	0.0	58.7	17.4	24.4	0.1	39.1	25.7	39.9	0.1
avg p@10	25.6	61.0	19.6	27.8	28.9	41.4	28.4	41.8	0.3
std p@10	36.8	1.3	1.4	2.0	9.7	1.6	1.5	1.1	0.1

Table 5.6: result of ten-run WGAN original for different random seed

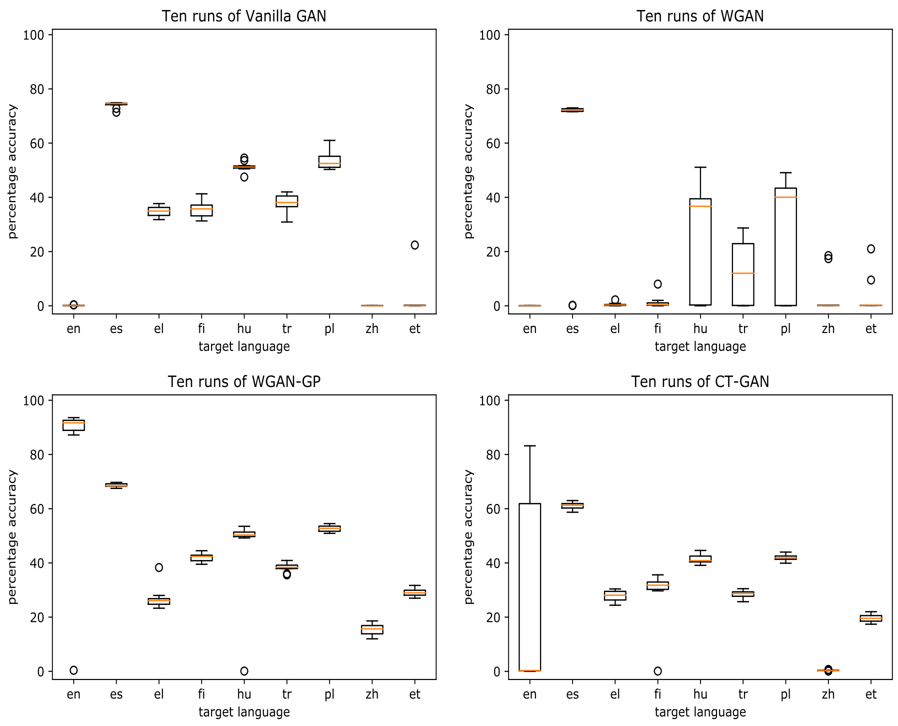

Figure 5.2: Box plot of ten-run

We can see that in the task of stability test, WGAN with gradient penalty works best and obtained very competitive result. The CT-GAN is the second robust model, and vanilla GAN is slightly better than WGAN.

5.4.2 Nearest neighbor translation table

In order to see how well our models performed on the real word translation task, we tested different types of nouns such as groups of animals, the name of locations and abstract nouns, also verbs and adjectives. We report the translations of some selected representative words("cat", "Denmark", "relation", "smoke" and "specific") for EN to EN, EN to ES, EN to ET and EN to EL. Since from the last section, we know that WGAN with gradient penalty is the most robust algorithm, we will only focus on it and compared to vanilla GAN.

tgt	**Vanilla GAN**
EN	respected, veteran, good, historian, senior, reputation, chief
	den, joseph, dem, dir, mit, carl, fred
	quite, very, extremely, equally, confident, fairly, seem
	publications, british, literature, history, publication, titled, recent
	terribly, quite, incredibly, seem, equally, extremely, frankly
ES	gato(cat), perro(dog), gorila(gorilla), conejo(rabbit),· · ·
	mapache(raccoon), zorro(fox), felis.
	dinamarca(Denmark), suecia(Sweden), noruega(Norway), finlandia(Finland), · · ·
	copenhague, danesa(Danish), escania.
	relaciona(relate), relacionar(relate), relacional(relational), relacionan(relate), · · ·
	concierne(it concerns), relación(relationship), correlación(correlation).
	humo(smoke), humos(fumes), fumar(smoke), cigarrillo(cigarette), · · ·
	arder(burn), inflamable(flammable), alquitrán(tar).
	específicas, específica, específicos, específico, · · ·
	determinadas, determinada, concretos.
ET	koer(dog), koera(dog), kassi(cat), kass(cat), · · ·
	koeri(dog), koeratõug(dog breed), koerad(dogs).
	taanis(in Denmark), norras(Norwegian), rootsis(Swedish), rootsit(Swedish), · · ·
	schleswigis(Schleswig), norraga(Norwegian), kopenhaagenis(Copenhagen).
	seose (relationship), seost (relationship), seos(the link), suhet(relationship), · · ·
	põhjuslikkus(causality), korrelatsiooni(correlation), vaadeldava(viewable).
	põlev(burning), põleva(burning), õhk(the air), süttib(lights up), · · ·
	põlemine(burning), põlevad(burning), põlemise(burning) .
	konkreetsele, konkreetse, konkreetsete, konkreetsel, konkreetses, · · ·
	konkreetset, konkreetsest (All 7 words are translated to "specific").
EL	ζώο(animal), σαύρες(lizards), κατοικίδιο(pet), ελάφι(deer), · · ·
	κουτάβια(puppies), σκύλο(dog), φιδιού(snake).
	δανία(Denmark), σουηδία(Sweden), δανίας(Danish), νορβηγία(Norway), · · ·
	σουηδίας(Swedish), νορβηγίας(Norwegian), ισλανδία(Iceland).
	συσχετίζει(correlates), συσχετίζεται(Associated), σχέση(relationship),· · ·
	συσχέτιση(correlation), σχετίζεται(related), αμοιβαιότητας(reciprocity), · · ·
	σχέσης(relationship).
	αέρας(air), καυσαέρια(exhaust gases), εισπνοή(inhalation), · · ·
	καπνό(tobacco), καπνός(tobacco), αέρα(air), ασφυξία(suffocation).
	συγκεκριμένων(specific), συγκεκριμένες(specific), συγκεκριμένη(specific), · · ·
	ανάλογα(accordingly), συγκεκριμένο(specific), συγκεκριμένους(specific), · · ·
	συγκεκριμένου(specific).

Table 5.7: translation of "cat", "Denmark", "relation", "smoke" and "specific", K = 7 (Vanilla GAN)

tgt	WGAN-GP
EN	cat, cats, dog, rabbit, kitten, pet, kitty
	denmark, norway, sweden, netherlands, copenhagen, finland, danish
	relation, relationship, relate, regard, analogous, namely, relating
	smoke, fumes, cigarette, smoking, fire, burning, soot
	specific, relevant, particular, appropriate, specifically, related, specify
ES	gato(cat), perro(dog), gorila(gorilla), cachorro(puppy), · · ·
	gatos(cats), ratón(mouse), conejo(rabbit).
	dinamarca(Denmark), suecia(Sweden), noruega(Norway), copenhague, · · ·
	finlandia(Finland), danesa(Danish), escania
	relaciona(relate), relacionar(relate), relación(relationship), · · ·
	concierne(it concerns), relacionan(relate), relacionada(related), respecto(respect)
	humo(smoke), humos(fumes), fumar(smoke), cigarrillo(cigarette),· · ·
	arder(burn), fuego(fire), inflamable(flammable).
	específica, específicas, específicos, específico (All 4 words are translated to specific), · · ·
	determinada(determined), concreta(concrete), determinadas(determined).
ET	kass(cat), koer(dog), koera(dogs), kassi(cat), koerad(dogs), · · ·
	koeratõug(dog breed), kategooria(category).
	taanis(in Denmark), norras(in Norway), rootsis(in Sweden), taani(Danish), · · ·
	kopenhaagenis(in Copenhagen),rootsit(Swedish), Schleswigis.
	seost(relationship), seose(relationship), seos(relationship), suhet (relationship),· · ·
	seosed(links), kirjeldamisega(description), võimalikkust(potential).
	suitsu(smoke), põleva(burning), süttib(lights up), õhku(air),· · ·
	põlev(burning), põlemine(burning), põlevad(burning).
	konkreetse, konkreetses, konkreetset, konkreetsele, konkreetsest, · · ·
	konkreetsete, konkreetsel (All 7 words are translated to "specific").
EL	σκύλο(dog), εξαφανίζεται(disappears), τραβάει(pulls), · · ·
	ανακατεύθυνση(redirected), ελάφι(deer), ζώο(animal), πρότυπο(standard).
	δανίας(of Denmark), νορβηγίας(Norwegian), σουηδίας(Swedish), ισλανδίας(Iceland), · · ·
	ολλανδίας(Netherlands), σουηδία(Sweden), νορβηγία(Norway).
	σχέση(relationship), συσχετίζει(correlates), συσχετίζεται(Associated), · · ·
	αναφορικά(with reference), συσχέτιση(correlation), σχετίζεται(related), · · ·
	σχέσης(relationship).
	καυσαέρια(exhaust fumes), φωτιά(fire), καπνό(tobacco), εισπνοή(inhalation),
	καπνός(tobacco), σύννεφα(Clouds), σκόνη(dust).
	συγκεκριμένες(specific), συγκεκριμένων(specific), συγκεκριμένο(specific), · · ·
	συγκεκριμένη(specific), ανάλογα(accordingly), συγκεκριμένου(specific), · · ·
	συγκεκριμένους(specific).

Table 5.8: translation of "cat", "Denmark", "relation", "smoke" and "specific", K = 7 (WGAN-GP)

In table 5.7 and 5.8, we can see that in the translation task of EN-EN, WGAN with gradient penalty works very good, and all translations are related, but the translations from vanilla GAN, as the table 5.2 and 5.3 indicate, all source words are randomly translated. For the other three language pars, they have similar performance.

On interest thing is the translation of "cat" on EN to EL from table 5.8, we see that there are irrelevant translations such as "disappears", "pulls", "standard" and "redirected". Thus we selected 20 extra different type words, varying from common to rarely used nouns, i.e, "dog", "bird", "crocodile", "lobster","book", "mathematics", "science", "education", "peach","forest","pest", "insect", "agriculture", "entity", "generosity", "absence", "emergency", "wisdom", "ghost", "Mediterranean", and "Jupiter". We found that the translations of all 20 words are relevant, even for the word "crocodile", the 7 closed translations are ύαινες(hyena), χελώνας(turtle), λιονταριού(lion), ερπετά(reptiles), φάλαινες (whales), κροκόδειλος (crocodile) and ερπετό(reptile).

5.4.3 Overview visualization

T-Distributed Stochastic Neighbor Embedding (T-SNE) is a dimensionality reduction technique, which is a non-linear manifold learning algorithm. It was developed by (Maaten et al. 2008). Compared to PCA, T-SNE more accurately captures the main information from high dimensional spaces than PCA does. However, T-SNE costs much more computational time than PCA, hence, to visualize the performance of all different GANs working on some language pairs, we first extract the most 150 relevant components from 300 by PCA, then transform those best 150 components to 2d space by T-SNE.

We randomly sampled 2000 points out of the most frequent 10,000 word embeddings from each of

- Original source embeddings before transformed (green dots).
- Source embeddings transformed by generator (blue dots).
- Target embeddings (red dots).

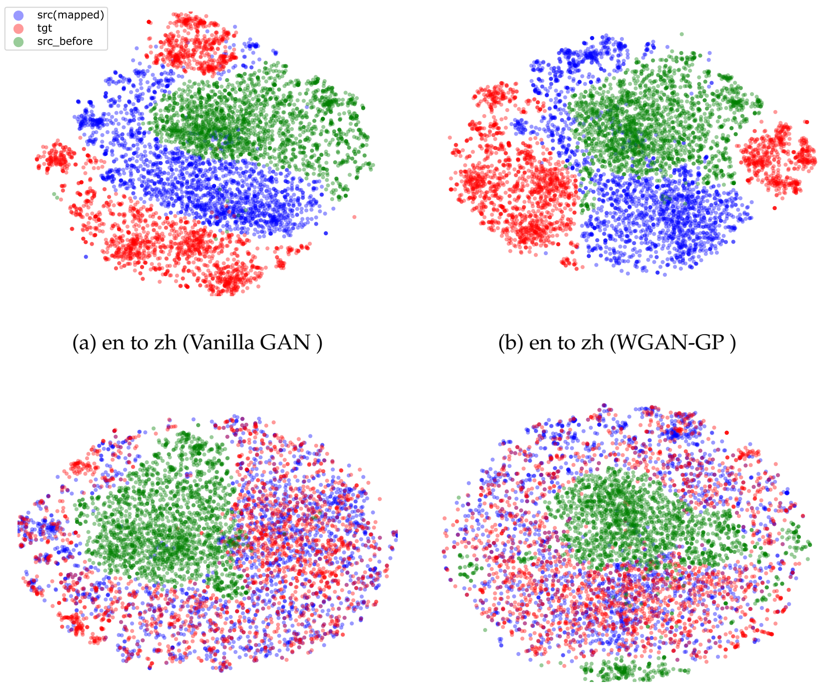

(a) en to zh (Vanilla GAN)

(b) en to zh (WGAN-GP)

(c) en to es (WGAN-GP)

(d) en to en (WGAN-GP)

Figure 5.3: 2d T-SNE after extract 150 components by PCA

For EN to ES and EN to EN, we can see that from figures 5.3(c) and (d), the translated English embeddings are mixed very well with target embeddings, but for English translate to largely different language such as Chinese as showed in the figures 5.3(a) and (b), from both the vanilla GAN and WGAN with gradient penalty, the discriminator successfully separate almost all samples, at least in the case of generator is a linear transformation.

Chapter 6

Discussion

From what we saw in the last section, we can in general conclude that our WGAN with gradient penalty model achieved the most powerful results compared to the other three GANs. We noticed that the English translate to English task is quite tricky, failed almost all of the times when attempted by vanilla GAN, WGAN and CT-GAN. Hartmann et al. (2018) explained that, in the case of vanilla GAN, the only probable reason that causes the task to fail is that the landscape of the discriminator's loss has fallen into a local optimum which makes the generator impossible to force the discriminator's loss out from it. For WGAN and CT-GAN, it could also be caused by the same issues which they illustrated.

Based on the results from the last section, we have a new explanation. In the translation of English to English task, both the source and target languages are the same, even when both embeddings are trained from a different corpus, or by different algorithms, the distributions of both word embeddings should be close to each other. By the properties of the linear transformation, the trained linear map by the generator can scale, rotate and reflect the source embeddings. Plus, the generator is a neural network and thus it will translate the source embeddings. Above with the word "translate" we mean shifting every point in the source space to another space in the same direction and distance. This implies that both distributions can either almost entirely be fitted together by the generator, or be separated by the discriminator, depending on the generator's learning ability. Based on the above, we can further deduce that to translate English to other languages which are not connected closely such as Estonian and Chinese, because the learning ability of the linear generator is limited, the linear generator can learn only part of the distribution of the target space. Figure 6.1 simply illustrates the concept of our explanation, where the red is the space of the source embedding, and blue is the target.

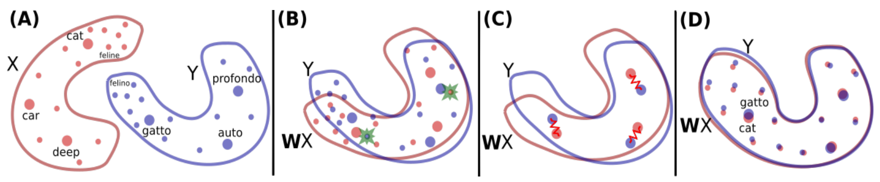

Figure 6.1: Figure 1 from Conneau et al [10]

To verify our hypothesis, we report the accuracy curves from the tasks of EN to EN, ES , ET and PL on figure 6.2. Figure 6.2(a) implies that our WGAN with gradient penalty models, during the min-max game, the generator is too strong that pushing almost all the source embeddings to fit the correct correspondings in target embeddings. Figure 6.2 also illustrates that once the generator successfully learned the distribution of target space, the discriminator almost impossible to split the entire source embeddings up.

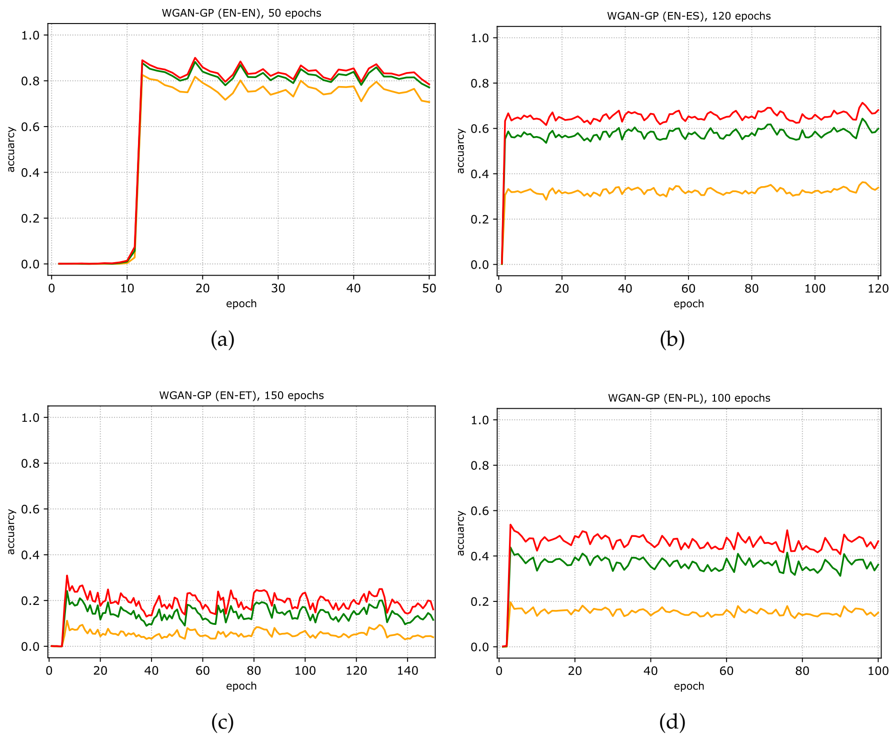

Figure 6.2: Accuracy curve from WGAN-GP

Furthermore, from the Figure 6.3(a),(b) and (d), we can see that in the EN to EN task, the loss curves of generators from the other three GANs, i.e., vanilla GAN, WGAN, and CT-GAN are quickly maximized, then almost unchanged afterward. This indicates that the generators are too weak that make the train procedures suffered by mode collapse. But Figure 6.3(c) shows that our WGAN with gradient penalty model did not experience this.

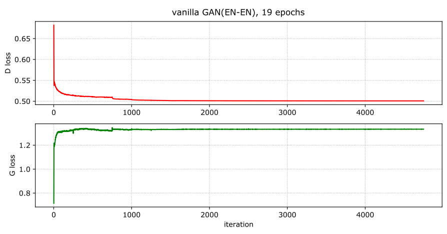

(a) vanilla GAN

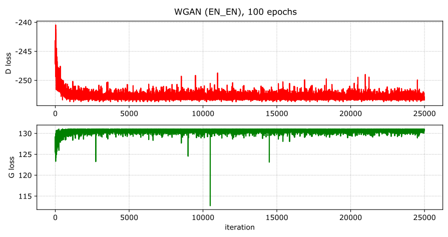

(b) WGAN

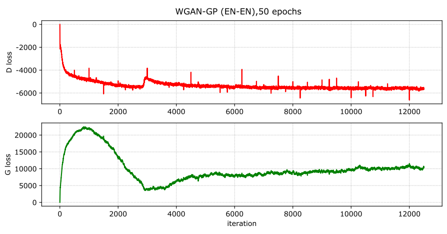

(c) WGAN-GP

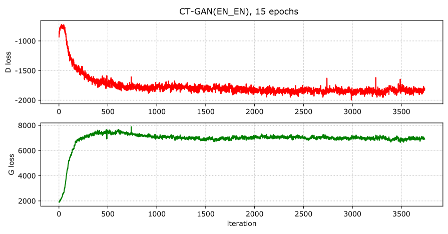

(d) CT-GAN

Figure 6.3: Loss curves from four different GANs (EN-EN)

Appendix A

Some deep learning techniques

A.1 Layer normalization

Training a deep neural network can cause internal covariate shift, i.e., the change of the input distribution of all layers. Especially for a deep neural network, even a small change can be expanded when the network goes deeper, therefore vanishing gradients can easily happen for saturating non-linearities. Batch normalization can help to reduce internal covariate shift by normalizing mini-batch input across their corresponding size. In particular,

$$\begin{aligned}
\mu_j &= \frac{1}{m}\sum_{j=1}^{n} \boldsymbol{x}_{ij} \\
\sigma_j^2 &= \frac{1}{m}\sum_{j=1}^{m} (\boldsymbol{x}_{ij} - \mu_i)^2 \\
\hat{\boldsymbol{x}} &= \frac{\boldsymbol{x}_{ij} - \mu_i}{\sqrt{\sigma^2 + \epsilon}},
\end{aligned}$$

where i indicates the index of example, and j is the index of feature. Thus the network converges relatively faster. The batch normalization method is proposed by Loffe et al. (2015).

Despite it achieving great success, batch normalization still has two main drawbacks:

- Model performance depends on the mini-batch size, because the mean and the variance ,which are calculated by mini-batch, cause errors and these errors will vary between different mini-batches.
- It's very difficult to apply to sequence models such as RNN.

Layer normalization is proposed by Ba et al. (2016). Unlike batch normalization, layer normalization does not depend on the size of the mini-batch, and also works well on RNNs. For each input example, it normalizes across features in a layer, more specifically,

$$\mu_i = \frac{1}{m}\sum_{j=1}^{m} \boldsymbol{x}_{ij}$$
$$\sigma_i^2 = \frac{1}{m}\sum_{j=1}^{m}(\boldsymbol{x}_{ij} - \mu_i)^2$$
$$\hat{\boldsymbol{x}} = \frac{\boldsymbol{x}_{ij} - \mu_i}{\sqrt{\sigma^2 + \epsilon}}$$

A.2 RMS prop

RMSprop is a optimization algorithm of gradient descent. It is proposed in the lecture 6 of Hinton et al [5] online course, and it is unpublisheded.

The motivation for developing RMSprop is to solve Adagrad's vanishing learning date problem. Unlike other gradient descent algorithm such as sgd or mini-batch gradient descent, by Ruder's explanation, Adagrad can adapts learning rate during training process, but the denominator term tends to zero after some training iterations. In particular, the RMSprop is

$$\mathbb{E}\left[\boldsymbol{g}^2\right]_t = 0.9\mathbb{E}\left[\boldsymbol{g}^2\right]_{t-1} + 0.1\boldsymbol{g}_t^2$$
$$\boldsymbol{w}_{t+1} = \boldsymbol{w}_t - \frac{\eta}{\sqrt{\mathbb{E}\left[\boldsymbol{g}^2\right]_t + \epsilon}}\boldsymbol{g}_t$$

where $\boldsymbol{g}$ is the gradient on tth iteration, η is the learning rate, and the ϵ is a small positive number to prevent division equals to zero. The learning rate divided by the mean of gradients which is exponentially decreasing. In Pytorch, the default values are: $\epsilon = 10^{-8}$.

A.3 Adam

Adam (Adaptive Moment Estimation) is another popular adaptive gradient descent algorithm, it proposed by Kingma et al. (2015). it combined both RMSprop and momentum, i.e. it not only compute and save the exponentially decaying of previous mean squared gradient, but also compute the previous momentum. More specifically,

$$m_t = \beta_1 m_{t-1} + (1-\beta_1)\boldsymbol{g}_t$$
$$v_t = \beta_2 v_{t-1} + (1-\beta_2)\boldsymbol{g}_t^2$$

[5] Neural Networks for Machine Learning

When m_t and v_t are initialized to zero vectors, Kingma et al. found that the they are unbiased. The final bias corrected terms are

$$\hat{m}_t = \frac{m_t}{1 - \beta_1^t}$$
$$\hat{v}_t = \frac{v_t}{1 - \beta_2^t}$$

combined both

$$\boldsymbol{w}_{t+1} = \boldsymbol{w}_t - \frac{\eta}{\sqrt{\hat{v}} + \epsilon}\hat{m}_t$$

Where the default settings in Pytorch are $\beta_1 = 0.9, \beta_2 = 0.999$ and $\epsilon = 10^{-8}$. In practice, Adam performs better than other adaptive gradient descent algorithm.

A.4 leaky Relu

The leaky Relu is an non-linear activation, which is developed by Maas et al. (2013). Since the normal Relu is $f(x) = \max(0, x)$, when $f(x)$ is negative, it's gradient will be zero. Therefore, if the output of $f(x)$ mostly are zeros, the normal Relu can cause vanishing gradients. The leaky Relu is to solve this problem by multiply a positive number which is greater than 1, more specifically,

$$f(x) = \begin{cases} x & x \geq 0 \\ \frac{x}{a} & 0 < x \end{cases}$$

where $a \in (1, +\infty)$, thus, the leaky Relu slightly change the gradient of the negative part of $f(x)$'s output, and make the backpropagation not suffered by vanishing gradients. The default setting in Pytorch is $\frac{1}{a} = 0.01$.

Appendix B

Theorems which support proofs

Smooth Urysohn's Lemma
Let $\mathcal{M}$ and $\mathcal{S}$ be two compact and disjoint subsets in a normal topological space $(\mathcal{X}, \mathcal{T})$, then there exists a function $f : \mathcal{X} \mapsto [0,1]$ which is smooth such that $f(x) = 0 \; \forall x \in \mathcal{S}$ and $f(x) = 1 \; \forall x \in \mathcal{M}$.

Lebesgue's Dominated Convergence Theorem.
Let $\{f_n\}$ be a sequence of real-valued measurable functions on a measure space (S, Σ, μ). Suppose that the sequence converges pointwise to a function f

$$\big|f_n(x)\big| \leq f(x)$$

for all the index number $n \in \mathbb{N}^+$ and $x \in S$, then f is integrable and

$$\lim_{n \to \infty} \int_S \big|f_n - f\big| d\mu = 0.$$

Radamacher's theorem
If U is an open subset in $\mathbb{R}^n$, $f : U \mapsto \mathbb{R}^m$ is Lipschitz continuous, then f is differentiable almost everywhere.

Bibliography

[1] Sebastian Ruder, Ivan Vulić, and Anders Søgaard. (2017). A Survey Of Cross-lingual Word Embedding Models. arXiv preprint arXiv:1706.04902.

[2] Tomas Mikolov, Kai Chen, Greg Corrado, and Jeffrey Dean. (2013). Efficient Estimation of Word Representations in Vector Space. arXiv preprint arXiv:1301.3781.

[3] Ian J.Goodfellow, Jean Pouget-Abadue, Mehdi Mirza, Bing Xu, David Warde-Farley, Sherjil ozair, Aaron Courville, and Yoshua Bengio. (2014). Generative Adversarial Nets. In Advances in neural information processing systems (pp. 2672-2680).

[4] Yanghua Jin, Jiakai Zhang, Minjun Li, Yingtao Tian, Huachun Zhu, and Zhihao Fang. (2017). Towards the Automatic Anime Characters Creation with Generative Adversarial Networks. arXiv preprint arXiv:1708.05509.

[5] Christian Ledig, Lucas Theis, Ferenc Huszar, Jose Caballero, Andrew Cunningham, Alejandro Acosta, Andrew Aitken, Alykhan Tejani, Johannes Totz, Zehan Wang, and Wenzhe Shi. (2016). Photo-Realistic Single Image Super-Resolution Using a Generative Adversarial Network. In Proceedings of the IEEE conference on computer vision and pattern recognition (pp. 4681-4690).

[6] Carl Vondrick, Hamed Pirsiavash, and Antonio Torralbai. (2016). Generating Videos with Scene Dynamics. In Advances In Neural Information Processing Systems (pp. 613-621).

[7] William Fedus, Ian Goodfellow, and Andrew M. Dai. (2018). MaskGAN: Better Text Generation via Filling in the______. In ICLR.

[8] Olof Mogren. (2016). C-RNN-GAN: Continuous recurrent neural networks with adversarial training. In Constructive machine learning workshop.

[9] Scott Reed, Zeynep Akata, Xinchen Yan, Lajanugen Logeswaran, Bernt Schiele, and Honglak Lee. (2016). Generative Adversarial Text to Image Synthesis. In ICML.

[10] Alexis Conneau, Guillaume Lample, Marc'Aurelio Ranzato, Ludovic Denoyer, and Hervé Jégou. (2018). Word Translation Without Parallel Data. In ICLR.

[11] Chao Xing, Dong Wang, Chao Liu, and Yiye Lin. (2015). Normalized Word Embedding and Orthogonal Transform for Bilingual Word Translation. In Proceedings of the 2015 Conference of the North American Chapter of the Association for Computational Linguistics: Human Language Technologies (pp. 1006-1011).

[12] Martin Arjovsky, Soumith Chintala, and Léon Bottou. (2017). Wasserstein GAN. arXiv preprint arXiv:1701.07875.

[13] Ishaan Gulrajani, Faruk Ahmed, Martin Arjovsky, Vincent Dumoulin, and Aaron Courville. (2017). Improved Training of Wasserstein GANs. Improved training of wasserstein gans. In Advances in Neural Information Processing Systems (pp. 5767-5777).

[14] Xiang Wei, Boqing Gong, Zixia Liu, Wei Lu, Liqiang Wang. (2018). Improving the Improved Training of Wasserstein GANs: A Consistency Term and Its Dual Effect. In ICLR.

[15] Tomas Mikolov, Quoc V. Le, and Ilya Sutskever. (2017). Exploiting Similarities among Languages for Machine Translation. arXiv preprint arXiv:1309.4168.

[16] Cédric Villani. (2008). Optimal transport, old and new. (Vol. 338). Springer Science & Business Media.

[17] Ishaan Gulrajani, Faruk Ahmed, Martin Arjovsky, Vincent Dumoulin and Aaron Courville. (2017). Improved Training of Wasserstein GANs. In Advances in Neural Information Processing Systems (pp. 5767-5777).

[18] Piotr Bojanowski, Edouard Grave, Armand Joulin, and Tomas Mikolov. (2016). Enriching Word Vectors with Subword Information. Transactions of the Association for Computational Linguistics, 5, pp.135-146.

[19] Martin Arjovsky and Léon Bottou. (2017). Towards Principled Methods for Training Generative Adversarial Networks. In ICLR.

[20] Hariharan Narayanan and Sanjoy Mitter. (2010). Sample complexity of testing the manifold hypothesis. In Advances in Neural Information Processing Systems (pp. 1786-1794).

[21] Miloš Radovanović, Alexandros Nanopoulos, and Mirjana Ivanović. (2010). Hubs in Space: Popular Nearest Neighbors in High-Dimensional Data. In Advances in Neural Information Processing Systems (pp. 1786-1794).

[22] Jeff Johnson, Matthijs Douze, and Hervé Jégou. (2017). Billion-scale similarity search with GPUs. arXiv preprint arXiv:1702.08734.

[23] Sergey Ioffe and Christian Szegedy. (2015). Batch Normalization: Accelerating Deep Network Training by Reducing Internal Covariate Shift. arXiv preprint arXiv:1702.08734.

[24] Anders Søgaard, Sebastian Ruder and Ivan Vulić. (2018). On the Limitations of Unsupervised Bilingual Dictionary Induction. In ACL.

[25] Jimmy Lei Ba, Jamie Ryan Kiros and Geoffrey E. Hinton. (2016). Layer Normalization. arXiv preprint arXiv:1607.06450.

[26] Sebastian Ruder. (2016). An overview of gradient descent optimization algorithms. arXiv preprint arXiv:1609.04747.

[27] Diederik P. Kingma and Jimmy Ba. (2015). Adam: A Method for Stochastic Optimization. In ICLR.

[28] Andrew L. Maas , Awni Y. Hannun and Andrew Y. Ng. (2013). Rectifier Nonlinearities Improve Neural Network Acoustic Models. In Proc. icml (Vol. 30, No. 1, p. 3).

[29] Laurens van der Maaten and Geoffrey Hinton. (2008). Visualizing data using t-SNE. Journal of machine learning research, 9(Nov), pp.2579-2605.

[30] Mareike Hartmann, Yova Kementchedjhieva and Anders Søgaard. (2018). Why is unsupervised alignment of English embeddings from different algorithms so hard? arXiv preprint arXiv:1809.00150.

[31] Jeffrey Pennington, Richard Socher and Christopher D. Manning. (2014). GloVe: Global Vectors for Word Representation In Proceedings of the 2014 conference on empirical methods in natural language processing (EMNLP) (pp. 1532-1543).